Diastereoselective Synthesis, Molecular Structure, and Solution Dynamics of *meso*- and *rac*-[Ethylenebis(4,7-dimethyl-η^5-1-indenyl)]zirconium Dichloride Isomers and Chain Transfer Reactions in Propene Polymerization with the *rac* Isomer

Luigi Resconi,* Fabrizio Piemontesi, Isabella Camurati, and Davide Balboni

Montell Italia, G. Natta Research Center, P.le G. Donegani 12, I-44100 Ferrara, Italy

Angelo Sironi and Massimo Moret

Dipartimento di Chimica Strutturale e Stereochimica Inorganica, Università di Milano, Via Venezian 21, 20133 Milano, Italy

Helena Rychlicki and Robert Zeigler

Montell U.S.A., Research & Development Center, 912 Appleton Road, Elkton, Maryland 21921

Received May 29, 1996[⊗]

The known *rac*-[ethylenebis(4,7-dimethyl-η^5-1-indenyl)]$ZrCl_2$ (**2r**) and its *meso* isomer (**2m**) have been compared with the prototypal chiral isospecific *rac*-[ethylenebis(η^5-1-indenyl)]-$ZrCl_2$ (**1r**) and its aspecific *meso* isomer **1m** in terms of molecular structures, solution dynamics, and ligand substitution effect on polymerization performance. In liquid propene at 50 °C, **2r**/MAO produces iPP with appreciably higher isotacticity but lower molecular weight and regiospecificity than **1r**/MAO. The lower molecular weight obtained with **2r** in liquid monomer is due to predominant chain transfer to the monomer after a secondary propene insertion, producing >90% *cis*-2-butenyl− end groups. At lower propene concentration, **2r**/MAO allows both β-hydrogen transfer after a primary insertion and β-methyl transfer. The low-activity **2m**/MAO catalyst produces low molecular weight aPP. The diastereoselective synthesis of **2r**,**m** via the corresponding *rac*- and *meso*-bis(4,7-dimethyl-1-(trimethylsilyl)-3-indenyl)ethane is reported. The crystal and molecular structures of *meso*-bis(4,7-dimethyl-1-(trimethylsilyl)-3-indenyl)ethane, **2r**,**m**, have been determined.

Introduction

It is now well established that in metallocene-catalyzed olefin polymerization all the details of polymer architecture are fully dictated by the π-ligand symmetry and spatial arrangement.[1] In the case of isotactic polypropene (iPP) synthesis, since the pioneering work of Ewen[2] and Kaminsky and Brintzinger,[3] impressive scientific and technological progress has been made. Proper ligand design has solved the quest for new chiral stereorigid, more stereospecific metallocenes via the modification of the C_2-symmetric, bridged bis-Cp ligand. Spaleck and co-workers[4] and Brintzinger and co-workers[5] have produced a large number of new isospecific *ansa*-zirconocenes which enable the synthesis of highly isotactic, high molecular weight polypropene. Isotacticity,[6,7] regioregularity,[8] and molecular weight[5,9] of iPP can be directly related to the ligand structure in terms of steric interactions of the incoming monomer with the active catalyst species.

To date, the best characterized zirconocene precatalyst is the C_2-symmetric, moderately isospecific *rac*-ethylenebis(1-indenyl)$ZrCl_2$ (*rac*-EBI$ZrCl_2$, **1r**), both in

[⊗] Abstract published in *Advance ACS Abstracts,* September 15, 1996.

(1) Ewen, J.; Elder, M.; Jones, R.; Haspeslagh, L.; Atwood, J.; Bott, S.; Robinson, K. *Makromol. Chem., Macromol. Symp.* **1991**, *48/49*, 253.

(2) (a) Ewen, J. *J. Am. Chem. Soc.* **1984**, *106*, 6355−6364. (b) Ewen, J. U.S. Patent 4,522,982 to Exxon, 1985. (c) Ewen, J. In Catalytic Polymerization of Olefins. *Studies on Surface Science Catalysis*; Keii, T., Soga, K., Eds; Elsevier: Amsterdam, 1986; Vol. 25, pp 271−292. (d) Ewen, J.; Haspeslagh, L.; Atwood, J.; Zhang, H. *J. Am. Chem. Soc.* **1987**, *109*, 6544−6545. (e) Ewen, J.; Haspeslagh, L.; Elder, M.; Atwood, J.; Zhang, H.; Cheng, H. In *Transition Metal Organometallic Catalysis and Olefin Polymerization*; Kaminsky, W., Sinn, H., Eds.; Springer-Verlag: Berlin, 1988; pp 281−289.

(3) (a) Kaminsky, W.; Külper, K.; Brintzinger, H.; Wild, F. *Angew. Chem., Int. Ed. Engl.* **1985**, *24*, 507−508. (b) Kaminsky, W.; Külper, K.; Buschermöhle, M.; Lüker, H. U.S. Patent 4,769,510 to Hoechst, 1988. (c) Kaminsky, W. *Angew. Makromol. Chem.* **1986**, *145/146*, 149−160. (d) Kaminsky, W. In *Catalytic Polymerization of Olefins*; Keii, T., Soga, K., Eds.; Elsevier: Amsterdam, 1986; pp 293−304.

(4) (a) Spaleck, W.; Antberg, M.; Rohrmann, J.; Winter, A.; Bachmann, B.; Kiprof, P.; Behm, J.; Herrmann, W. *Angew. Chem., Int. Ed. Engl.* **1992**, *31*, 1347−1350. (b) Spaleck, W.; Küber, F.; Winter, A.; Rohrmann, J.; Bachmann, B.; Antberg, M.; Dolle, V.; Paulus, E. *Organometallics* **1994**, *13*, 954.

(5) Stehling, U.; Diebold, J.; Kirsten, R.; Röll, W.; Brintzinger, H.-H.; Jüngling, S.; Mülhaupt, R.; Langhauser, F. *Organometallics* **1994**, *13*, 964−970.

(6) (a) Corradini, P.; Guerra, G.; Vacatello, M.; Villani, V. *Gazz. Chim. Ital.* **1988**, *118*, 173. (b) Cavallo, L.; Guerra, G.; Oliva, L.; Vacatello, M.; Corradini, P. *Polym. Commun.* **1989**, *30*, 16. (c) Cavallo, L.; Corradini, P.; Guerra, G.; Vacatello, M. *Polymer* **1991**, *32*, 1329. (d) Cavallo, L.; Guerra, G.; Vacatello, M.; Corradini, P. *Chirality* **1991**, *3*, 299.

(7) (a) Castonguay, L.; Rappé, A. *J. Am. Chem. Soc.* **1992**, *114*, 5832. (b) Hart, J.; Rappé, A. *J. Am. Chem. Soc.* **1993**, *115*, 6159. (c) Kawamura-Kuribayashi, H.; Koga, N.; Morokuma, K. *J. Am. Chem. Soc.* **1992**, *114*, 8687.

(8) Guerra, G.; Cavallo, L.; Moscardi, G.; Vacatello, M.; Corradini, P. *J. Am. Chem. Soc.* **1994**, *116*, 2988.

(9) Jüngling, S.; Mülhaupt, R.; Stehling, U.; Brintzinger, H. H.; Fischer, D.; Langhauser, F. *J. Polym. Sci.: Part A: Polym. Chem.* **1995**, *33*, 1305.

S0276-7333(96)00423-2 CCC: $12.00

Chart 1

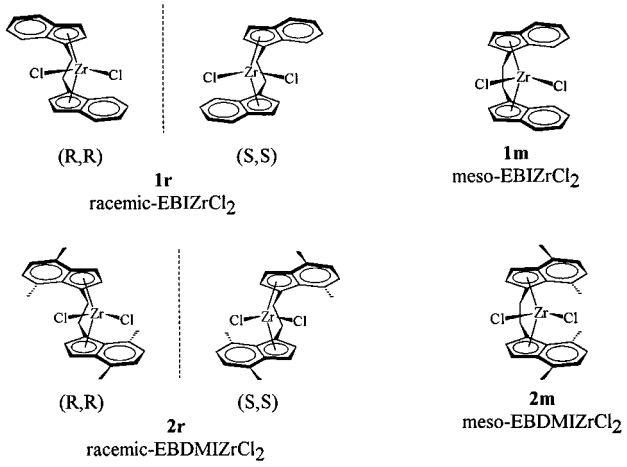

terms of its synthesis,[10] molecular characterization[11] and performance in propene polymerization.[12,13] In particular, the mechanistic details of chain propagation, chain transfer, and chain isomerization reactions[12−14] of **1r**/MAO have been disclosed. Because of the large set of data now available, **1r** serves as an excellent benchmark for mechanistic studies.

Collins and co-workers[10d] and the Hoechst group[15] recently reported on the synthesis of several ethylene-bridged bis(indenyl)zirconium dichlorides bearing substituents on the ligand phenyl rings, including *rac*-[ethylenebis(4,7-dimethyl-1-indenyl)]$ZrCl_2$ (*rac*-EBDMI$ZrCl_2$, **2r**; Chart 1), and on their behavior in MAO-cocatalyzed polymerizations, but the results obtained with **2r**/MAO in propene polymerization, e.g. lower activities and much lower iPP molecular weights in comparison to **1r**, were not rationalized in terms of the polymerization mechanism. Before these reports appeared, we had synthesized **2r** and its stereoisomer, *meso*-EBDMI$ZrCl_2$ (**2m**), and investigated their behavior toward olefin polymerization.

Although propene polymerization performance of **2r** turned out[10d,15] to be poorer than we expected, our investigation of the **2r**/MAO and **2m**/MAO systems in the polymerization of 1-olefins provided us with a better understanding of the chain transfer mechanisms and eventually led us to the discovery of two new, highly active catalyst systems for the production of a wide range of ethylene-based polymers.[16] In this paper we report the crystal and molecular structures of **2r**,**m** and their diastereoselective synthesis and discuss our results on propene polymerization with **2r**/MAO and **2m**/MAO.

Scheme 1. Isomers and Byproducts Isolated and Identified in the Synthesis of 1,2-Bis(4,7-dimethylindenyl)ethane

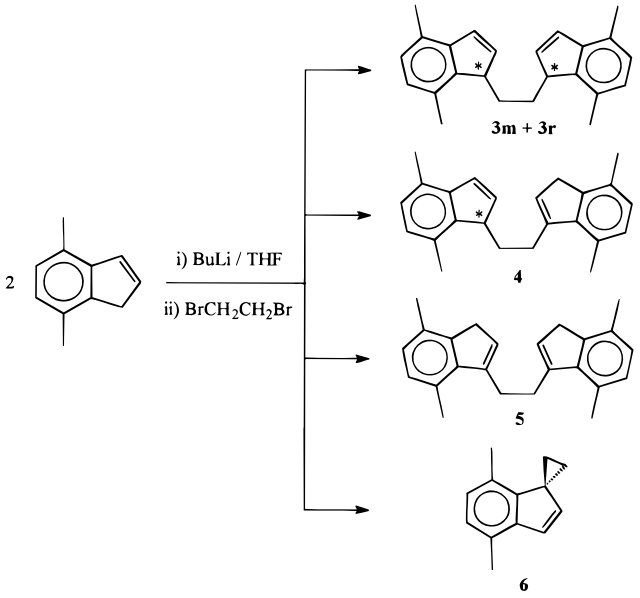

Results and Discussion

Synthesis of *rac*/*meso*-[Ethylenebis(4,7-dimethyl-1-indenyl)]$ZrCl_2$. The synthesis of 4,7-dimethylindene is described in the literature.[17] The synthesis of 1,2-bis(4,7-dimethylindenyl)ethane from the Li salt of 4,7-dimethylindene and 1,2-dibromoethane in THF gives a higher yield than the corresponding synthesis of 1,2-bis(indenyl)ethane (a 62% yield has been reported by the Hoechst group[15]). All possible isomers were obtained (Scheme 1).

All isomers **3**−**5** undergo double deprotonation with KH in THF to give the ligand dianion. Isomers **3** and **4** are isomerized to **5** by heating in DMSO with KOH or by quenching the dipotassium salt (generated with KH in THF) with MeOH.

By comparison of the spectra, the ^1H NMR resonances of the three isomers **3m**,**r**, **4**, and **5** and the spiro derivative **6** were assigned (Scheme 2).

Among the reasons that led us to the choice of the ethylenebis(4,7-dimethyl-1-indenyl) ligand in the first place, there was the hope that methyl substitution in the 7,7′ positions would inhibit the formation of the (usually) undesired *meso* isomer (which, being achiral, produces atactic polypropene[2a,18]) due to an expected unfavorable steric interaction between the two methyl

(10) (a) Wild, F.; Wasiucionek, M.; Huttner, G.; Brintzinger, H. H. *J. Organomet. Chem.* **1985**, *288*, 63. (b) Collins, S.; Kuntz, B.; Taylor, N.; Ward, D. *J. Organomet. Chem.* **1988**, *342*, 21. (c) Grossman, R.; Doyle, R. A.; Buchwald, S. *Organometallics* **1991**, *10*, 1501. (d) Lee, J.; Gauthier, W.; Ball, J.; Iyengar, B.; Collins, S. *Organometallics* **1992**, *11*, 2115.

(11) Piemontesi, F.; Camurati, I.; Resconi, L.; Balboni, D.; Sironi, A.; Moret, M.; Zeigler, R.; Piccolrovazzi, N. *Organometallics* **1995**, *14*, 1256.

(12) (a) Drögemüller, H.; Niedoba, S.; Kaminsky, W. *Polym. React. Engin.* **1986**, 299. (b) Tsutsui, T.; Kashiwa, N.; Mizuno, A. *Makromol. Chem., Rapid Commun.* **1990**, *11*, 565. (c) Huang, J.; Rempel, G. *Stud. Surf. Sci. Catal.* **1992**, *73*, 169. (d) Fisher, D.; Jüngling, S.; Mülhaupt, R. *Makromol. Chem., Macromol. Symp.* **1993**, *66*, 191.

(13) Resconi, L.; Fait, A.; Piemontesi, F.; Colonnesi, M.; Rychlicki, H.; Zeigler, R. *Macromolecules* **1995**, *28*, 6667 and references therein. Resconi, L.; Piemontesi, F.; Camurati, I.; Rychlicki, H.; Colonnesi, M.; Balboni, D. *Polym. Mater. Sci. Engin.* **1995**, *73*, 516.

(14) (a) Busico, V.; Cipullo, R.; Corradini, P. *Makromol. Chem., Rapid Commun.* **1993**, *14*, 97. (b) Busico, V.; Cipullo, R. *J. Am. Chem. Soc.* **1994**, *116*, 9329. (c) Busico, V.; Cipullo, R.; Chadwick, J. C.; Modder, J. F.; Sudmeijer, O. *Macromolecules* **1994**, *27*, 7538. (d) Leclerc, M. K.; Brintzinger, H. H. *J. Am. Chem. Soc.* **1995**, *117*, 1651.

(15) Winter, A.; Antberg, M.; Dolle, V.; Rohrmann, J.; Spaleck, W. Eur. Pat. Appl. 537 686 (U.S. Pat. 5,304,614) (to Hoechst), 1993.

(16) Resconi, L.; Galimberti, M.; Piemontesi, F.; Guglielmi, F.; Albizzati, E. Eur. Pat. Appl. 575 875 (to Spherilene), 1993. Resconi, L.; Piemontesi, F.; Galimberti, M. Eur. Pat. Appl. 643 078 (to Spherilene), 1995. Dall'Occo, T.; Resconi, L.; Balbontin, G.; Albizzati, E. PCT Int. Appl. WO 95 35,333 (to Spherilene), 1995.

(17) Herz, W. *J. Am. Chem. Soc.* **1953**, *75*, 73. Piccolrovazzi, N.; Pino, P.; Consiglio, G.; Sironi, A.; Moret, M. *Organometallics* **1990**, *9*, 3098. Reuschling, D.; Rohrmann, J.; Erker, G.; Nolte, R.; Aulbach, M.; Weiss, A. U.S. Patent 5,194,619 (to Hoechst), 1993. Coe, J. W.; Vetelino, M. G.; Kemp, D. S. *Tetrahedron Lett.* **1994**, *35* (36), 6627. Erker, G.; Psiorz, C.; Fröhlich, R.; Grehl, M. *Tetrahedron* **1995**, *51*, 4347.

(18) Collins, S.; Gauthier, W.; Holden, D.; Kuntz, B.; Taylor, N.; Ward, D. *Organometallics* **1991**, *10*, 2061.

Scheme 2

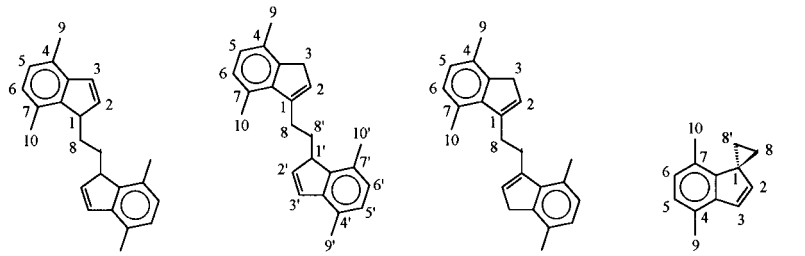

	3r + 3m	**4**	**5**	**6**
^{1}H NMR (δ, ppm, $CDCl_3$, r.t.):				
H1	m 3.49-3.59	-	-	
H2	d,d 6.47 (J=1.66, 5.4)	bs 6.15	s 6.31	d 6.08, 6.06 (J=5.61)
H3	n.a.	bs 3.00-3.16	s 3.21	d 6.91, 6.88 (J=5.61)
H5, 6	6.71-7.11	6.71-7.11	d 7.02, 6.98 (J=7.68)	d 6.96, 6.93 (J=7.68)
			d 6.95, 6.91 (J=7.68)	d 6.82, 6.79 (J=7.68)
H9, 10	s 2.20, s 2.35	s 2.40, s 2.50	s 2.59, s 2.35	s 2.42, s 2.25
H8	n.a.	n.a.	s 3.12	m 2.06, 2.08, 2.09, 2.12
				m 1.49, 1.51, 1.52, 1.55
H1'		m 3.60-3.75		
H2'		d,d 6.7 (J= 1.66, 5.4)		
H3'		n.a.		
H9',10'		s 2.29, s 2.38		

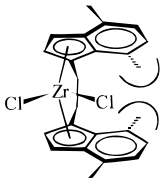

Figure 1. Unfavorable 7,7′ methyl−methyl contacts expected for **2m**.

groups in 7,7′ for the *meso* isomer (Figure 1). This interaction is obviously absent in the racemic isomer. Concurrent formation of the aspecific *meso* isomer in the synthesis of racemic *ansa*-metallocenes is a recurring problem.[19]

We assumed that the structure of *meso*-EBDMIZrCl_2 (**2m**) would be the same as that observed for *meso*-EBIZrCl_2 (**1m**)[11] and *meso*-ethylenebis(4,5,6,7-tetrahydro-1-indenyl)ZrCl_2 (*meso*-EBTHIZrCl_2).[18] However, the addition of methyl groups in 7,7′ had no beneficial effect on the *rac*/*meso* selectivity: although Collins obtained a 25% yield of the pure *rac* isomer by reaction of the dilithium salt of 1,2-bis(4,7-dimethylindenyl)-ethane with $ZrCl_4$ in dimethoxyethane,[10d] Winter et al. reported a 59% yield of a 3:1 *rac*:*meso* isomer distribution, by carrying out the reaction in THF with slow, simultaneous addition of the two reactants dissolved in THF.[15] The pure racemic isomer was obtained by crystallization from toluene/pentane, presumably in very low yield.

By using Buchwald's protocol,[10c] we obtained *rac*:*meso* ratios of 2.3:1 for EBDMIZrCl_2 (room-temperature synthesis), very similar to that reported by Buchwald (and confirmed in our studies) for EBTHIZrCl_2, and of 1:1 (room temperature) and 1:10 (−70 °C) for Me_2Si-(4,7-dimethyl-1-indenyl)ZrCl_2. The reason for the unexpected formation of relevant amounts of the *meso* isomers of both zirconocenes bearing the strapped bis-(4,7-dimethyl-1-indenyl) ligands becomes clear upon inspection of the crystal structure of *meso*-EBDMIZrCl_2 (**2m**), which is discussed below together with the crystal structure of *rac*-EBDMIZrCl_2 (**2r**).

Given our interest in both isomers of **2**,[16] and the lack of a high-yield, *diastereoselective* synthesis for their large-scale production, we have developed a different method based on the use of the bis(trimethylsilyl)-derivative of bis(4,7-dimethylindenyl)ethane.

Our method is based on a modification of the high-yield synthesis under mild conditions of *ansa*-metallocenes from Me_3Sn- and Et_3Sn-derivatized ligands developed by Nifant'ev.[20] Lisowsky[21] similarly reported the high-yield synthesis of **1** via the bis(1-(tributylstannyl)-3-indenyl)ethane intermediate, prepared in turn from the Mg salt of bis(indenyl)ethane. The isolated yield was 85% of the 1:1 mixture of isomers.

The use of trialkyltin chlorides (toxic and of high molecular weight) is, however, not without drawbacks: for example in the case of **1**, 2 mol (0.483 kg) of triethyltin chloride has to be recycled or disposed of per 1 mol (0.418 kg) of product.

The development by Nifant'ev prompted us to evaluate the use of $SiMe_3$ as the leaving group. The use of Cp′$SiMe_3$ as reagent in the synthesis of both Cp′MCl_3 and Cp′$_2MCl_2$ is well-known.[22] We are aware of only one example of the use of bridged bis-Cp′$SiMe_3$ ligands for zirconocene synthesis, which has been reported in the literature during our investigation.[23]

Despite the requirement of one additional step (the transformation of the ligand dianion into the bis-$SiMe_3$ derivative) with respect to the direct synthesis of *ansa*-zirconocenes via the Li or K salts of their ligands, this approach offers several advantages over the classic method:

1. The prolonged handling of the ligand dianion is not required, as the dilithium or dipotassium salt is immediately quenched with Me_3SiCl to generate the air-stable bis-$SiMe_3$ derivative.

(19) See for example the discussion in: (a) Ellis, W.; Hollis, T.; Odenkirk, Whelan, J.; Ostrander, R.; Rheingold, A.; Bosnich, B. *Organometallics* **1993**, *12*, 4391 and references therein. (b) Huttenloch, M.; Diebold, J.; Rief, U.; Brintzinger, H. H.; Gilbert, A.; Katz, T. *Organometallics* **1992**, *11*, 3600 and references therein.

(20) Nifant'ev, I. E.; Ivchenko, P. V.; Resconi, L. Eur. Pat. Appl. 722 950 (to Montell), 1996. Nifant'ev, I. E.; Ivchenko, P. V. *Organometallics*, in press.

(21) Lisowsky, R. EPA 669 340 to Witco, 1995.

(22) Winter, C. H.; Zhou, X.-X.; Dobbs, D. A.; Heeg, M. J. *Organometallics* **1991**, *10*, 210.

(23) Hafner, K.; Mink, C.; Lindner, H. J. *Angew. Chem., Int. Ed. Engl.* **1994**, *33*, 1479.

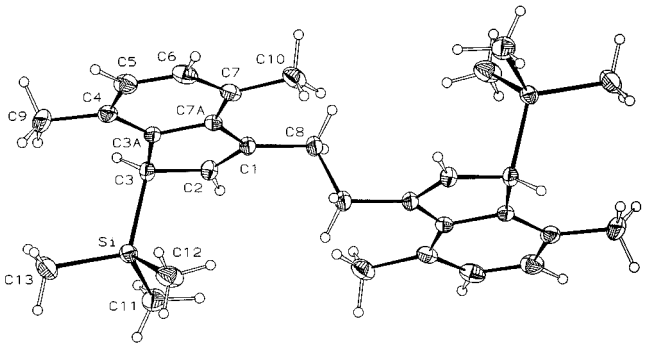

Figure 2. ORTEP view of bis(3-(trimethylsilyl)-4,7-dimethylindenyl)ethane. Hydrogen atoms were given arbitrary radii. Thermal ellipsoids have been drawn at the 30% probability level.

Scheme 3

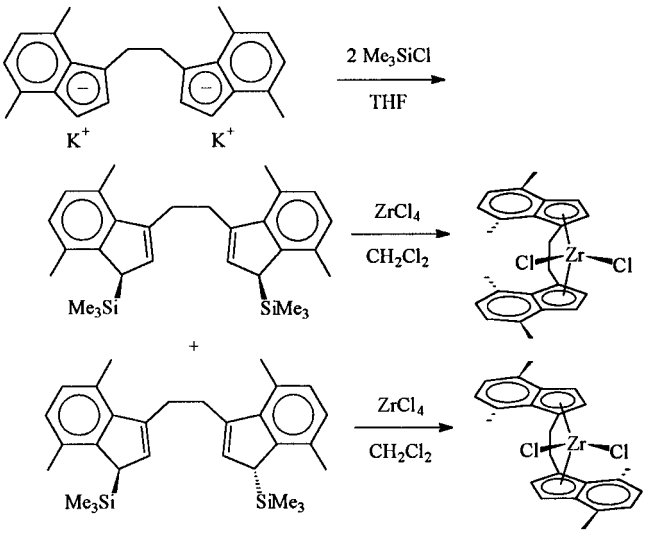

2. Although THF has to be used in the synthesis of the bis-$SiMe_3$ derivative, the metalation step is carried out in the low-boiling, nonflammable CH_2Cl_2 solvent and under much higher concentration, thus minimizing the amount of solvent required.

3. The purification step is much simpler. In all known procedures the raw product has to be extracted with CH_2Cl_2 in order to remove insoluble byproducts. In our case, all byproducts are soluble; hence, only a washing step with the appropriate solvent is required to produce the final product in high purity.

4. Our method (as in the case of Nifant'ev's procedure via SnR_3 derivatives) offers the unique opportunity to become highly diastereoselective, as the bridged bis-$SiMe_3$ derivatives, having 2 stereogenic carbons, are obtained as both the *meso* and *rac* isomers: the *meso* isomer produces the *meso*-zirconocene and the *rac* isomer produces the *rac*-zirconocene with complete diastereoselectivity (Scheme 3).

With the use of the bis(trimethylsilyl)derivative of bis-(4,7-dimethylindenyl)ethane for the synthesis of **2r**,**m** we have achieved both high yields and high diastereoselectivity. The *meso* isomer of [ethylenebis(4,7-dimethylindenyl)]zirconium dichloride (**2m**), which previously could only be obtained as a minor byproduct of the (low yield) synthesis of **2r**, can now be produced with high yields (80%) and high chemical and isomeric purity (>99%).

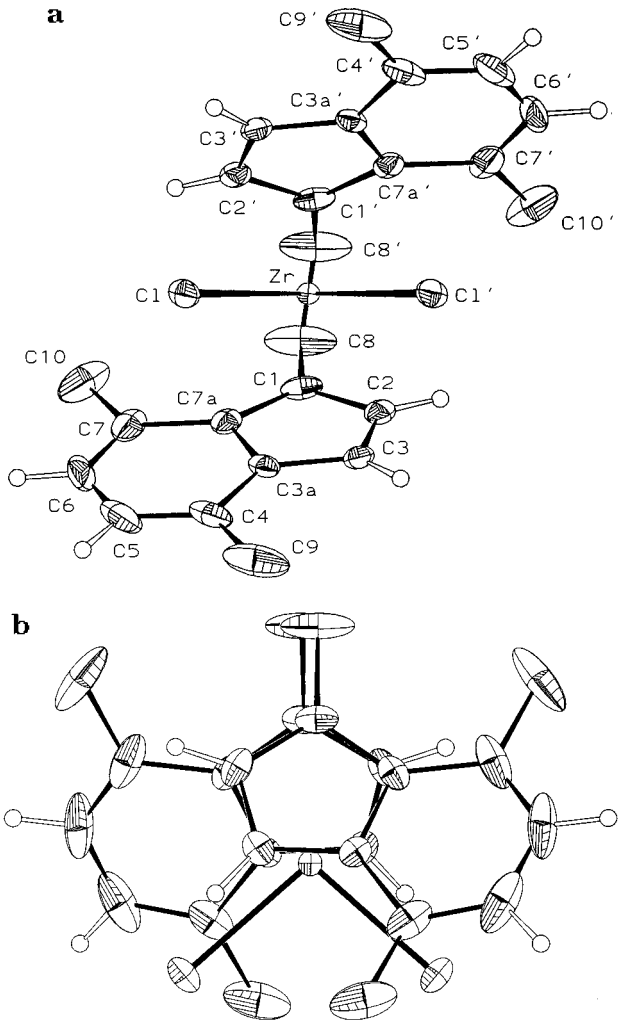

Figure 3. ORTEP view of **2r**: (a) with labeling, viewed down the Cl−Zr−Cl bisector; (b) top view. Hydrogen atoms were given arbitrary radii. Thermal ellipsoids have been drawn at the 30% probability level. Primed atoms refer to symmetry-equivalent atoms with the ($-x$, y, $0.5 - z$) symmetry operation.

This selectivity is of course subject to the possibility of easy ligand isomer separation. In the case of bis-(4,7-dimethyl-1-(trimethylsilyl)-3-indenyl)ethane, the *rac* isomer is readily dissolved in pentane, leaving the pure *meso* isomer that can be further purified by extraction in hot hexane.

The ligand isomeric distribution can be determined by ^1H or ^{13}C NMR in $C_2D_2Cl_4$ at 120 °C, as the two isomers have identical spectra in $CDCl_3$ at room temperature. Their structure was assigned by resolving the molecular structure of the *meso* isomer, which readily crystallizes from either CH_2Cl_2 or Et_2O.

Crystal and Molecular Structures of *meso*-1,2-Bis(4,7-dimethyl-1-(trimethylsilyl)-3-indenyl)ethane, *rac*-[Ethylenebis(4,7-dimethyl-η^5-1-indenyl)]-zirconium Dichloride (2r), and *meso*-[Ethylenebis-(4,7-dimethyl-η^5-1-indenyl)]zirconium Dichloride (2m). Figure 2 shows an ORTEP plot of *meso*-bis(4,7-dimethyl-1-(trimethylsilyl)-3-indenyl)ethane while Figures 3 and 4 show two different ORTEP views of **2r** and **2m**, respectively. Tables 1 (lengths), 2 (angles), and 3 (least-squares planes and slip-fold indicators) contain the most relevant bonding parameters for the three compounds.

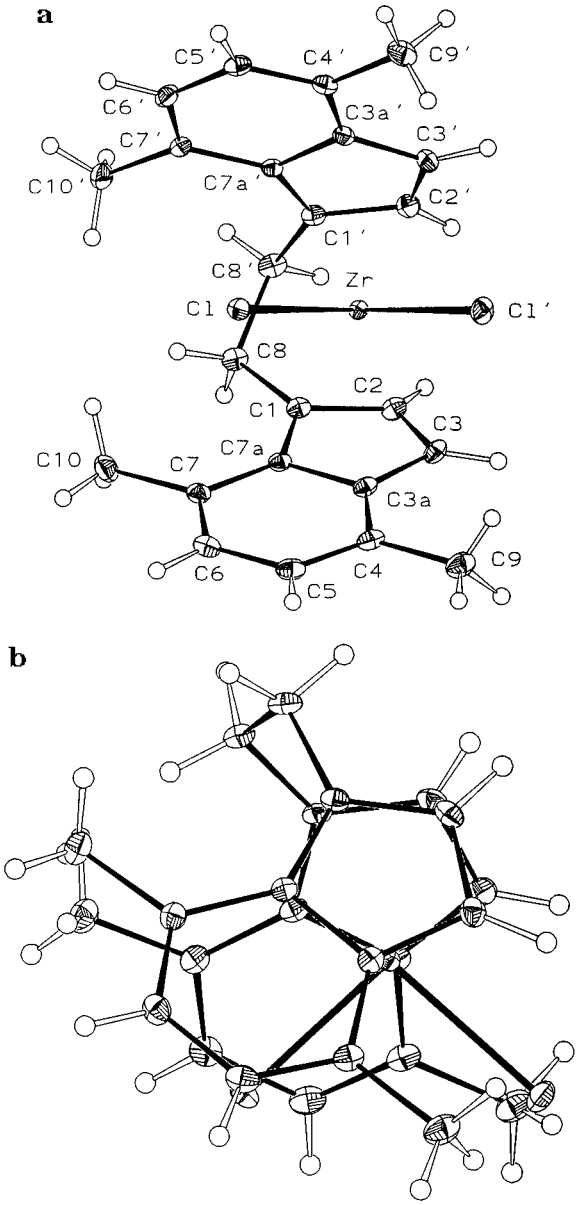

Figure 4. ORTEP view of **2m**: (a) with labeling, viewed down the Cl−Zr−Cl bisector; (b) top view. Hydrogen atoms were given arbitrary radii. Thermal ellipsoids have been drawn at the 30% probability level. Atoms and primed atoms are not related by symmetry.

The *meso*-bis(4,7-dimethyl-1-(trimethylsilyl)-3-indenyl)ethane molecule has a crystallographically imposed C_i symmetry and, judging from the observed volume per non-hydrogen atom (21.8 Å^3), is poorly packed even if the "residual" volume, not leaving any space for clathrated solvent molecules, is well distributed. The observed pattern of bond distances and angles is consistent with the double bond character of the C(1)−C(2) bond and with a substantially delocalized picture of the benzene ring. The three Si−Me bond lengths are very similar (average 1.855 Å) and substantially shorter than the fourth Si−C bond distance (Si−C(3), 1.918(3) Å), which is elongated because of the steric repulsion between the $SiMe_3$ and the dimethylindenyl moiety. Steric effects are also responsible for the observed symmetry breaking in the C−C−C bond angle pattern of the indenyl system, which would be expected to have substantially C_s symmetry according to Domenicano's rules.[24] Indeed, the actual pattern of C−C−C bond angles clearly shows that the $SiMe_3$ group, lying below the plane of the benzene ring, is less effective than the

Table 1. Bond Lengths (Å)[a]

	meso-EBDMI(TMS)$_2$	**2r**	**2m** I	**2m** II
Zr−Cl		2.4236(7)	2.4105(4)	2.4505(4)
Zr−C(1)		2.494(3)	2.462(2)	2.498(2)
Zr−C(2)		2.458(3)	2.489(2)	2.475(2)
Zr−C(3)		2.522(3)	2.513(2)	2.501(2)
Zr−C(3a)		2.618(3)	2.596(2)	2.584(2)
Zr−C(7a)		2.586(3)	2.599(2)	2.602(2)
Si−C(3)	1.918(3)			
Si−C(11)	1.859(4)			
Si−C(12)	1.853(4)			
Si−C(13)	1.853(3)			
C(1)−C(2)	1.335(4)	1.388(5)	1.419(3)	1.416(3)
C(1)−C(7a)	1.475(4)	1.436(5)	1.444(2)	1.441(2)
C(1)−C(8)	1.518(3)	1.503(5)	1.512(2)	1.514(2)
C(2)−C(3)	1.485(3)	1.379(5)	1.405(3)	1.399(3)
C(3)−C(3a)	1.497(3)	1.395(5)	1.430(3)	1.419(2)
C(3a)−C(4)	1.391(3)	1.441(4)	1.428(2)	1.430(2)
C(3a)−C(7a)	1.418(3)	1.435(5)	1.437(2)	1.446(2)
C(4)−C(5)	1.383(4)	1.345(7)	1.361(3)	1.353(3)
C(4)−C(9)	1.506(4)	1.491(9)	1.497(3)	1.505(3)
C(5)−C(6)	1.381(5)	1.42(1)	1.415(3)	1.411(3)
C(6)−C(7)	1.386(4)	1.348(7)	1.363(3)	1.372(2)
C(7)−C(7a)	1.403(4)	1.446(4)	1.433(2)	1.431(2)
C(7)−C(10)	1.510(4)	1.509(9)	1.500(3)	1.496(3)
C(8)−C(8′)	1.523(5)	1.412(9)	1.543(3)	

[a] I, II indicate atoms (I) and primed (II) atoms of **2m** as shown in Figure 4a. Primes address primed atoms (II) in **2m** and symmetry-equivalent atoms for **2r** ($-x$, y, $0.5 - z$) and *meso*-1,2-bis(1-(trimethylsilyl)-4,7-dimethyl-3-indenyl)ethane ($1 - x$, $-y$, $1 - z$).

Table 2. Selected Bond and Torsional Angles (deg)[a]

	meso-EBDMI(TMS)$_2$	**2r**	**2m** I	**2m** II
cp−Zr−*cp*′		125.3(1)	123.8(1)	
Cl−Zr−Cl′		97.48(5)	95.91(2)	
cp−Zr−Cl		107.1(1)	107.3(1)	106.7(1)
cp−Zr−Cl′		108.2(1)	109.5(1)	109.9(1)
C(3)−Si−C(11)	108.3(2)			
C(3)−Si−C(12)	108.6(2)			
C(3)−Si−C(13)	112.9(2)			
C(11)−Si−C(12)	109.2(2)			
C(11)−Si−C(13)	107.0(2)			
C(12)−Si−C(13)	110.8(2)			
C(2)−C(1)−C(8)	122.8(2)	124.3(5)	123.4(2)	122.7(2)
C(7a)−C(1)−C(2)	108.6(2)	107.0(3)	106.7(2)	106.5(1)
C(7a)−C(1)−C(8)	128.6(2)	128.6(5)	129.8(2)	130.8(2)
C(1)−C(2)−C(3)	112.4(2)	110.6(3)	109.8(2)	110.6(2)
C(2)−C(3)−C(3a)	102.1(2)	107.9(3)	107.6(2)	107.4(2)
C(2)−C(3)−Si	106.3(2)			
C(3a)−C(3)−Si	112.1(2)			
C(7a)−C(3a)−C(3)	109.0(2)	108.3(3)	108.0(1)	108.2(1)
C(7a)−C(3a)−C(4)	121.6(2)	123.7(4)	121.9(2)	121.4(2)
C(3)−C(3a)−C(4)	129.3(2)	128.0(4)	130.0(2)	130.4(2)
C(3a)−C(4)−C(5)	116.6(3)	114.0(5)	116.4(2)	116.9(2)
C(4)−C(5)−C(6)	122.0(3)	124.1(6)	122.0(2)	122.2(2)
C(5)−C(6)−C(7)	122.8(3)	123.0(5)	123.6(2)	123.6(2)
C(7a)−C(7)−C(6)	116.2(3)	117.2(5)	116.8(2)	116.6(2)
C(1)−C(7a)−C(3a)	107.1(2)	106.2(3)	107.4(1)	107.2(1)
C(1)−C(7a)−C(7)	132.3(2)	135.8(4)	133.5(2)	133.5(2)
C(3a)−C(7a)−C(7)	120.6(2)	117.9(4)	119.1(2)	119.3(1)
C(1)−C(8)−C(8′)−C(1′)	180.0	9.6(9)	−42.4(2)	
bz−*cp*−*cp*′−*bz*′		142.2(1)	−14.5(1)	

[a] *cp* and *bz* refer to the center of mass of the five- and six-membered rings of the indenyl ligands. I, II indicate atoms (I) and primed (II) atoms of **2m** as shown in Figure 4a. Primes address primed atoms (II) in the *meso*-derivative and symmetry-equivalent atoms ($-x$, y, $0.5 - z$) in the *rac*-derivative.

(24) Domenicano, A.; Vaciago, A.; Coulson, C. A. *Acta Crystallogr., Sect. B* **1975**, *31*, 221.

Table 3. Angles between Relevant Least-Squares Planes and Slip-Fold Parameters

		2m	
	2r	I	II
al/*bz* (deg)	5.5(2)	8.6(1)	6.7(1)
$ZrCl_2$/*in* (deg)	31.42(6)	33.36(3)	31.79(3)
in/*in*′ (deg)	62.14(8)	65.14(3)	
Ψ (deg)	4.21	3.82	3.56
Ω (deg)	1.56	6.25	3.94
Δ (Å)	0.164	0.148	0.138

[a] *al*, *bz*, *in*, and $ZrCl_2$ refer to the least-squares planes defined by the allylic moieties (C(1), C(2), C(3)), the six-membered rings, the indenyl ligands, and the $ZrCl_2$ atoms, respectively. I, II indicate atoms (I) and primed (II) atoms of **2m** as shown in Figure 3b. Primes address primed atoms (II) in the *meso*-derivative and symmetry-equivalent atoms ($-x$, y, $0.5 - z$) in the *rac*-derivative.

"*ansa*" methylene, which lies in the plane of the benzene ring, in perturbing the indenyl moiety (C(3)−C(3a)−C(4) 129.3(2)° vs C(1)−C(7a)−C(7) 132.3(2)°; C(4)−C(3a)−C(7a) 121.6(2) vs C(7)−C(7a)−C(3a) 120.6(2)°).

This is the first structural characterization of the *rac*- and *meso*-ethylene(dimethylindenyl)$_2$M fragments. Unfortunately the crystal structure determination of **2r**, which has a crystallographically imposed C_2 symmetry, is affected by some disorder and the bonding parameters are not accurate enough to allow a detailed comparison of the fragment in the two different conformations. The fact that both **2r** and **2m** are not isomorphous to the corresponding isomers of **1**[11] (even if the *rac* complexes share the same space group and have similar cell parameters) suggests that the methyl substitution is a major perturbation to the molecules' self-recognition. Interestingly, it is now the *rac* derivative (and not the *meso*- as it is the case of **1**) that has the less efficient packing (i.e. the higher volume per molecule) and is slightly disordered. However, similarly to what happens to the two stereoisomers of **1**, it is the less-bound system (in the solid state) that has the larger conformational freedom (*i.e.* to be disordered).

In both **2r** and **2m** the presence of the *ansa* bridge determines a marked asymmetry of the indenyl moieties which can be addressed by the same angles used to discuss the conformation of *meso*-bis(4,7-dimethyl-1-(trimethylsilyl)-3-indenyl)ethane, namely, C(3)−C(3a)−C(4) vs C(1)−C(7a)−C(7) and C(4)−C(3a)−C(7a) vs C(7)−C(7a)−C(3a), which are 128.0(4)° vs 135.8(4)° and 123.7(4)° vs 117.9(4)° in **2r** and 130.2° vs 133.5° and 121.6° vs 119.2° in **2m** (averaged values).

In both **2r** and **2m** the Zr−C bond interactions involving the bridgehead carbon atoms are longer than the other carbon−metal bonds within the η^5-moiety. Incipient $\eta^5 \rightarrow \eta^3$ distortions are normally observed for η^5-indenyl complexes and are commonly measured by the so-called slip-fold parameters Ψ, Ω, and Δ defined in ref 25. As for the two EBIZrCl$_2$ stereoisomers, on moving from *rac* to *meso*, the indenyl ligands take more room around the Zr atom as evidenced by the shrinking of Cl−Zr−Cl angle and the lengthening of the average Zr−Cl bond distance. Moreover, since the two Zr−Cl bonds in the *meso* derivative are not related by symmetry and, more importantly, their local environments are dissimilar, they are markedly different. However, in the present case, the *cp*−Zr−*cp*′ angle in the *meso* derivative is smaller than that in the *rac* derivative because of the corresponding widening of the *cp*−Zr−Cl′ angles. This is correlated to the marked rotation, about the *cp*−Zr vector, of the two indenyl moieties which brings the *ansa* ethane bridge, in the *meso* derivative, almost *trans* to Cl′. Such an impressive asymmetric location of the bridge with respect to the Cl−Zr−Cl′ moiety has been recently attributed in *ansa*-titanocene complexes to *intra*molecular repulsion of the π-bonded carbon atoms (and their β-H) with the Cl ligands. This is clearly not the case for zirconocene derivatives where the larger size of the Zr atom, with respect to Ti, forces longer M−Cl and M−C bonds and, consequently, longer Cl···C and Cl···H *intra*molecular contacts. Accordingly, we do not observe, in the *meso* derivative, any "anomalous" Cl···C or Cl···H *intra*molecular contact, and we must conclude that the observed conformation must be due to *intra*molecular interactions *within* the "organic" *ansa*-bridged ligand, given the "external" constraint of the substantially rigid coordination sphere at the Zr centers. In other words, what these molecules have in common is actually the local stereochemistry at the Zr atom while the substituents of the *ansa*-bridged ligand, in the present case the four methyl groups, drive the rotations about the *cp*−Zr and C(8)−C(8′) bond in order to reach the overall best conformation compatible with the Zr *pseudo*-tetrahedral coordination. Such substantial conformational freedom about the *cp*−Zr bonds is what allows the unexpected formation of relevant amounts of the *meso* isomer.

The *rac* stereoisomer, reported in Figure 3, according to an adaptation by Schlogl of the Cahn−Ingold−Prelog rules has clearly an *S*,*S* configuration of the bridgehead carbon atoms and a λ conformation of the Zr,C(1),C(8),C(8′),C(1′) "metallacycle". Conversely the *meso* stereoisomer reported in Figure 4 has λ,*R*,*S* stereochemistry. However, both in solution and in the solid state, as they crystallize in a centrosymmetric space group, their enantiomers (δ,*R*,*R* and δ,*S*,*R*, respectively) are also present.

NMR Analysis and Solution Conformation of 2r,m. Ethylene-bridged *ansa*-metallocenes can exist in two limit conformations,[26] which we named Π and Y.[11] We found that for **1r** at room temperature, Π and Y are almost (60:40) equiprobable, with $\Delta H_{\Pi Y} = 0.945$ kcal/mol.[11] The method of analysis proposed in ref 11 was followed to investigate the solution behavior of **2r**,**m**. Their ^{1}H NMR spectra are compared in Figure 5.

^{1}H and ^{13}C NMR spectral assignments are reported in Table 4, with atom labeling according to Figures 3 and 4. The assignments are based on bidimensional COSY[27] and NOESY[28] spectra (see the Supporting Information for details). The DEPT-45, XH-CORR,[29] and COLOC[30] spectra of **2r** enabled us to identify all the carbons. This was not possible for the *meso* isomer owing to its low solubility leading to a poor signal to

(25) Faller, J. W.; Crabtree, R. H.; Habib, A. *Organometallics* **1985**, *4*, 929.

(26) Brintzinger, H. H. In *Transition Metals and Organometallics as Catalysts for Olefin Polymerization*; Kaminsky, W., Sinn, H., Eds.; Springer-Verlag: Berlin, 1988; p 249.

(27) (a) Aue, W. P.; Bartholdi, E.; Ernst, R. R. *J. Chem. Phys.* **1976**, *64*, 2229. (b) Nagayama, K.; et al. *J. Magn. Reson.* **1980**, *40*, 321.

(28) States, D. J.; Haberkorn, R. A.; Ruben, D. J. *J. Magn. Reson.* **1982**, *48*, 286.

(29) Bax, A.; Morris, G. *J. Magn. Reson.* **1981**, *42*, 501.

(30) Kessler, H.; Griesinger, C.; Zarbock, J; Loosli; H. R. *J. Magn. Reson.* **1984**, *57*, 331.

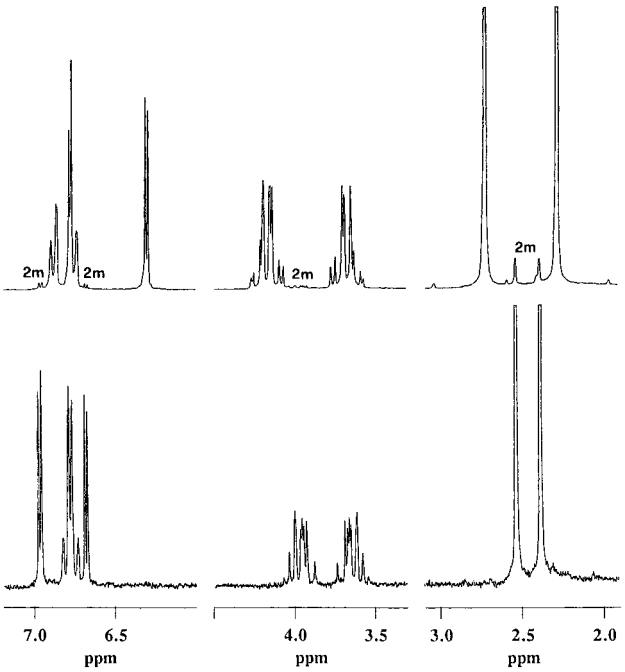

Figure 5. ^{1}H NMR spectrum of **2r** (top) and **2m** (bottom) in CD_2Cl_2 at room temperature.

Table 4. Carbon and Proton Assignments for 2r,m

	^{1}H NMR[a]		^{13}C NMR[a]	
atom	**2r**	**2m**	**2r**	**2m**
1			121.49	108.65
2	6.28	6.97	112.66	106.85
3	6.80	6.68	113.38	100.42
3a			128.68	117.37 or 116.99[b]
4			132.94	121.86 or 123.02[b]
5	6.91	6.76	125.37	114.89
6	6.77	6.80	128.42	118.85
7			130.12	121.86 or 123.02[b]
7a			125.17	117.37 or 116.99
8A	3.5−3.8	3.5−3.8	30.28	21.99
8B	4.0−4.3	3.8−4.1		
9	2.30	2.38	18.62	8.65
10	2.71	2.53	21.38	10.63

[a] Solvent CD_2Cl_2. [b] Indeterminate assignments.

noise ratio in the COLOC spectrum. Therefore some uncertainty remains in the carbon assignments for **2m**.

The solution behavior of **2r** was investigated by acquiring ^{1}H NMR from 50 to 120 °C in $C_2D_2Cl_4$ and focusing our attention on the bridge protons. These protons form an AA′BB′ spin system, whose pattern depends on the values of chemical shift difference ($\Delta\delta$) and coupling constants (J), that can be obtained simulating the spectrum with a computer program (PANIC, from Bruker).

The values of $\Delta\delta$ and J (geminal ^2J and vicinal ^3J) are reported in Table 5. The vicinal coupling constants are the most sensitive to conformational changes as they depend on the dihedral angle θ between the protons according to the Karplus relation:

$$^3J = 7.23 - 0.51 \cos\theta + 5.16 \cos 2\theta$$

In the presence of conformational equilibrium we observe an averaging of the J values between the two limit conformations $^3J_{obs} = aJ_\Pi + bJ_Y$, where a and b are the relative residence times for each conformation and J_Π and J_Y are the limit vicinal coupling constants.

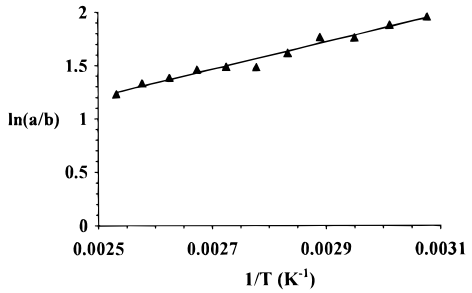

Figure 6. Linear correlation of ln(a/b) vs 1/T (Arrhenius plot) for **2r**.

Table 5. VT-NMR Data for 2r: Experimental Coupling Constants and Chemical Shift Differences ($\Delta\delta$)

T (K)	$\Delta\delta$ (Hz)	^2J (Hz)	^3J(AB′) (Hz)	^3J(BB′) (Hz)	^3J(AA′) (Hz)
395	0.417	−14.76	7.50	4.20	9.75
388	0.419	−14.81	7.51	4.12	9.88
381	0.422	−14.88	7.45	4.16	9.97
374	0.425	−14.84	7.49	4.08	10.06
367	0.429	−14.71	7.31	4.02	10.20
360	0.433	−14.73	7.39	3.91	10.18
353	0.436	−14.71	7.30	4.03	10.37
346	0.440	−14.60	7.32	3.74	10.55
339	0.445	−14.67	7.22	3.63	10.62
332	0.449	−14.68	7.10	3.67	10.81
325	0.453	−14.69	7.40	3.56	10.71

Table 6. VT-NMR Data for 2r: Calculated Coupling Constants and Residence Times

T (K)	a (mol fract)	b (mol fract)	^3J(AB′) (Hz)	^3J(BB′) (Hz)	^3J(AA′) (Hz)
395	0.226	0.774	7.50	4.44	9.75
388	0.209	0.791	7.51	4.30	9.88
381	0.200	0.800	7.45	4.26	9.97
374	0.188	0.812	7.49	4.14	10.06
367	0.185	0.815	7.31	4.17	10.20
360	0.185	0.815	7.39	4.13	10.18
353	0.166	0.834	7.30	4.02	10.37
346	0.146	0.854	7.32	3.82	10.55
339	0.147	0.853	7.22	3.85	10.62
332	0.132	0.868	7.10	3.78	10.81
325	0.124	0.876	7.39	3.58	10.71

Following the method reported in ref 11 we obtained the results reported in Table 6. **2r** appears to be more rigid than **1r** as at 52 °C one conformation is present in larger amount (87.6%). As previously assumed for **1r**,[11] the more stable conformation should be Π (indenyl forward) due to interactions between the methyl groups in the 7 and 7′ positions and the ethylene bridge. This fact can not be directly confirmed from the NMR spectrum, but the molecular mechanics calculations performed by Rappé[7b] support our assumption. Kaminsky[31] described the dynamic behavior of **1r** and *rac*-ethylenebis(2,4,7-trimethyl-1-indenyl)zirconium dichloride and presented molecular mechanics calculations showing the presence of two equiprobable conformations for **1r** (in agreement with our experimental results[11]) and only one (Π) for the trimethyl derivative.

The Arrhenius plot (Figure 6) according to the equation ln(a/b) = $\Delta H_{\Pi Y}/RT$ gives a $\Delta H_{\Pi Y}$ = 2.55 kcal/mol for **2r** (standard error = 0.09 kcal/mol, R = 0.995). A similar freezing of the Π → Y conformational exchange has been achieved by Rieger on ethylene bridged un-

(31) Kaminsky, W.; Rabe, O.; Schauwienold A.-M.; Schupfner, G. U.; Hanss, J.; Kopf, J. *J. Organomet. Chem.* **1995**, *497*, 181.

Table 7. Propene Polymerization with *rac*-Zirconocene/MAO Catalysts[a]

sample no.	zirconocene[b]	amt of Zr (μmol)	Al/Zr (M)	yield (g)	$\bar{M}_V$[c]	T_m[d] (°C)
1	*rac*-EBIZrCl$_2$	0.48	8000	74.5	34500	136
2	*rac*-EBTHIZrCl$_2$	0.47	19000	17.4	29300	137
3	rac-EBDMIZrCl$_2$	2.07	2000	156.7	7300	131
4	*rac*-Me$_2$SiInd$_2$ZrCl$_2$	0.22	38000	44.1	56000	144
5	*rac*-Me$_2$Si-(H$_4$Ind)$_2$ZrCl$_2$	1.09	8000	58.8	30300	148
6	Me$_2$Si(4,7-Me$_2$-Ind)$_2$ZrCl$_2$[e]	1.98	4000	27.1	17800	

[a] Polymerization conditions: 1-L stainless-steel autoclave, propene 0.4 L, 50 °C, 1 h, zirconocene/MAO aged 10 min in 10 mL of toluene. [b] EBI = ethylenebis(indenyl), EBTHI = ethylenebis(4,5,6,7-tetrahydroindenyl), EBDMI = ethylenebis(4,7-Me$_2$Ind). [c] Calculated from the experimental intrinsic viscosities $[\eta]_{(THN,\ 135\ °C)}$ according to the $[\eta] = K\bar{M}_V^{\alpha}$ with $K = 1.93 \times 10^{-4}$ and $\alpha = 0.74$.[48] [d] Melting point and heat of fusion determined from the second melting, scan rate 10 °C/min. [e] Contains 16% *meso* isomer.

symmetric zirconocenes, by substituting one of the bridge hydrogens with a phenyl group.[32]

2m, as found for **1m**,[11] is expected to be in a rapid interconversion equilibrium between two equienergetic (equiprobable mirror images) conformers. This is confirmed by the analysis of the AA′BB′ spin system of the bridge protons[33] as already at room temperature the values of the vicinal J (^3J(AB′) = 6.98 Hz; ^3J(BB′) = 6.95 Hz; ^3J(AA′) = 7.05 Hz) are those expected for a 1:1 mixture.

Propene Polymerization with *rac*-EBDMIZrCl$_2$ (2r). 1. Catalyst Performance in Liquid Monomer. According to the model of Guerra and Corradini,[6] the substitution pattern on the ethylenebis(4,7-dimethylindenyl) ligand could be expected to increase both the rigidity and the stereoselecting ability of the catalytic complex, resulting in a higher isospecificity. As a matter of fact, Collins and co-workers have shown that **2r** is more isospecific than either the unsubstituted **1r** or ethylenebis(5,6-dimethylindenyl)ZrCl$_2$.[10d]

Hart and Rappé[7b] performed molecular mechanics analysis of nonbonded interactions in propene insertion on a large set of alkyl-substituted *rac*-(ethylenebis-(indenyl))(2,4,6-trimethylheptyl)zirconium species, providing realistic estimates of the $\Delta\Delta G^{\ddagger}$ for correct versus wrong enantioface insertion. Their values confirmed that **2r** should be more isospecific than **1r**. Catalyst regiospecificity however was not discussed in either work. As the different catalysts were tested under a single set of experimental conditions (toluene solution, 3 bar of propene, 40 °C), no kinetic or thermodynamic parameters were obtained. Due to the likely presence of growing-chain-end epimerization which could disguise the actual isospecificity of a zirconocene catalyst, we have compared the catalytic performance of **2r** with **1r** and several other C_2-symmetric, moderately isospecific *ansa*-zirconocenes in *liquid monomer* under our standard polymerization conditions (prereacted catalyst/cocatalyst, 50 °C, 1 h). The results are reported in Tables 7 and 8.

Table 8. ^{13}C NMR Characterization of iPP Samples from Different Metallocenes

sample no.	tacticity (%)[a] b	m	mmmm	regioinversions (%)[b] 2,1 E	2,1 T	3,1	f(2,1)[c] (%)
1	0.9725	94.65	86.99	0.35	0.19	traces	0.69
2	0.9824	96.54	91.50	0.1	traces	0.8	0.9
3	0.9831	96.48	91.36	1.26	0.41	0.05	2.75
4	0.9798	96.04	90.30	0.27	0.21	0	0.48
5	0.9896	97.94	91.39	0.14	0	0.40	0.54
6[d]	0.9822	96.50	91.39	1.01	0.41	0	1.44

[a] Determined by assuming the enantiomorphic site model; see ref 13. [b] Internal erythro (E), threo (T), and isomerized 3,1 regioinverted units determined as described in ref 13. [c] Total secondary insertions including end groups. $f(2,1) = \%\ 2,1_{int}/100 + 2,1_{term}/P_n$. [d] *n*-Pentane-insoluble fraction.

Confirming Collins' results, we found that also in liquid monomer at 50 °C, compared to the parent catalyst **1r**/MAO, the system **2r**/MAO is less active and produces a much lower molecular weight iPP. On the other side, **2r**, with an enantioface selectivity value $b_{50\ °C} = 0.9831$ (producing iPP with 91% mmmm pentad content), is appreciably more stereospecific than **1r**, which has $b_{50\ °C} = 0.9725$ (that is 87% mmmm pentad content).

Interestingly, along with the above features, **2r** is also markedly less regiospecific than **1r**, producing iPP with a total of 1.7% secondary units[34] versus 0.6% with **1r**.[13] Note that the same general differences are observed between the *rac*-Me$_2$Si(Ind)$_2$ZrCl$_2$/MAO and *rac*-Me$_2$Si-(4,7-Me$_2$Ind)$_2$ZrCl$_2$/MAO systems (entries 4−6 in Tables 7 and 8).

As to what is the driving force to secondary insertions, Rappè[7b] has calculated that, in the 4,4′-dimethyl substitution pattern, there would be an unfavorable, direct steric interaction between the ligand methyl in the 4′ position and the methyl of a primary propene monomer coordinated with the wrong enantioface. The same steric interaction very likely is the cause for a higher rate of secondary insertions.

The presence of a relatively high amount of regioirregularities is the key to understanding the polymerization behavior of **2r**.

In fact, the lower activity of the **2r**/MAO catalyst is easily ascribed to the higher frequency of such secondary insertions, as it has been demonstrated that secondary chain ends effectively slow subsequent monomer insertion.[35,36] In the case of **2r**, the presence of detectable amounts of 3,1 units (arising from *unimolecular* isomer-

(32) Rieger, B.; Jany, G.; Fawzi, R.; Steimann, M. *Organometallics* **1994**, *13*, 647.

(33) In effect each conformer of **2m** lacks any element of symmetry, and therefore the bridge protons form an ABCD spin system. If a rapid conformational equilibrium between the two conformers exists, this spin system degenerates into the simpler AA′BB′.

(34) (a) Soga, K.; Shiono, T.; Takemura, S.; Kaminsky, W. *Makromol. Chem., Rapid Commun.* **1987**, *8*, 305. (b) Grassi, A.; Zambelli, A.; Resconi, L.; Albizzati, E.; Mazzocchi, R. *Macromolecules* **1988**, *21*, 617. (c) Grassi, A.; Ammendola, P.; Longo, P.; Albizzati, E.; Resconi, L.; Mazzocchi, R. *Gazz. Chim. Ital.* **1988**, *118*, 539. (d) Cheng, H.; Ewen, J. *Makromol. Chem.* **1989**, *190*, 1931. (e) Tsutsui, T.; Ishimaru, N.; Mizuno, A.; Toyota, A.; Kashiwa, N. *Polymer* **1989**, *30*, 1350. (f) Tsutsui, T. Mizuno, A.; Kashiwa, N. *Makromol. Chem.* **1989**, *190*, 1177. (g) Tsutsui, T.; Kioka, M.; Toyota, A.; Kashiwa, N. In *Catalytic Olefin Polymerization*; Studies on Surface Science and Catalysis, Vol. 56; Keii, T., Soga, K., Eds.; Elsevier: Amsterdam, 1990; p 493. (h) Rieger, B.; Chien, J. *Polym. Bull.* **1989**, *21*, 159. (i) Rieger, B.; Mu, X.; Mallin, D.; Rausch, M.; Chien, J. *Macromolecules* **1990**, *23*, 3559. (j) Chien, J.; Sugimoto, R. *J. Polym. Sci. A: Polym. Chem.* **1991**, *29*, 459. (k) Mizuno, A.; Tsutsui, T.; Kashiwa, N. *Polymer* **1992**, *33*, 254. The correct nomenclature for these structures should be secondary *meso* and secondary *rac*. We use here Zambelli's nomenclature,[34b] erythro (*E*) and threo (*T*), respectively, to avoid confusion with the m, r dyad definition. We rename the isomerized 4-methylene unit as 3,1 instead of 1,3, according to the suggestion of Busico: Busico, V.; Cipullo, R. *J. Organomet. Chem.* **1995**, *497*, 113.

ization of secondary units[13]) even in liquid monomer further confirms the site-obstructing effect of a secondary chain end toward insertion, an effect that becomes overwhelming in the case of tetrahydroindenyl ligands, such as in *rac*-ethylenebis(tetrahydroindenyl)$ZrCl_2$ and *rac*-$Me_2Si(H_4Ind)_2ZrCl_2$ (entries 2 and 5 in Table 8).

Also the lower molecular weights produced by both **2r** and *rac*-$Me_2Si(4,7\text{-}Me_2Ind)_2ZrCl_2$ in comparison to their unsubstituted parent compounds are fully accounted for by secondary insertions (see below).

2. Chain Transfer Reactions. End-group analysis of low molecular weight poly(α-olefins) from metallocene catalysts has shown that monomer insertion at metallocene active centers is largely primary (occasional isolated secondary units are also observed with most chiral zirconocenes) and chain transfer mostly occurs via β-hydrogen transfer after a primary insertion (with the formation of *n*-propyl and vinylidene end groups[37]) which can be both unimolecular (β-hydrogen transfer to the metal) and bimolecular (β-hydrogen transfer to the monomer). The relative rates of the two transfer reactions are a function of monomer concentration.[9,13]

In highly substituted zirconocenes (in all cases reported so far, zirconocenes bearing Cp ligands with substituents in all four frontal positions), unimolecular β-methyl transfer has also been observed.[37c,38]

Recent studies on chain transfer mechanisms have unveiled a more complicated picture than previously realized.[9,13] In addition to vinylidene, 2-butenyl end groups have also been detected in iPP made with zirconocenes with no alkyl substituent in the 2 position of the indenyl rings, such as in the *rac*-ethylenebis(tetrahydroindenyl)$ZrCl_2$/MAO[39] and **1r**/MAO catalysts[40] at low polymerization temperatures. Mülhaupt and co-workers[9] (for the catalyst system *rac*-Me_2Si(benzindenyl)$_2ZrCl_2$/MAO) and ourselves[13] (for the catalyst system *rac*-EBI$ZrCl_2$/MAO at 50 °C) have recently reported that their presence at high monomer concentrations indicates that the main chain transfer pathway becomes methylene β-hydrogen transfer to a coordinated propene monomer after an isolated *secondary* insertion.

Furthermore, we had assigned the stereochemistry of the terminal double bond as cis based on both its ^{13}C NMR peak positions and inspection of molecular models.[13] **2r**, because of the very low molecular weight iPP it produces, provides an excellent model catalyst for studying the kinetics of the different elementary steps in chain transfer reactions.

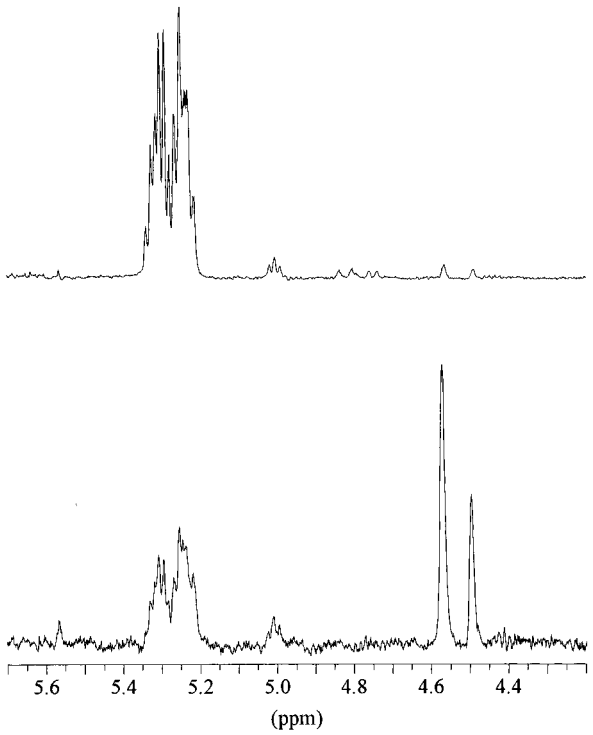

Figure 7. ^1H NMR spectrum of the olefin region of iPP sample 3 obtained from **2r**/MAO (top) and iPP sample 1 from **1r** (bottom).

In the case of iPP produced with **2r**/MAO in liquid propene at 50 °C, the *cis*-2-butenyl end group accounts for 90% of all unsaturated end groups, while for **1r** we found a 60/40 ratio of *cis*-2-butenyl vs vinylidene end groups by ^1H NMR (Figure 7).

Vinylidene end groups become relevant at lower monomer concentrations. More interestingly, also the allyl groups become detectable and account for up to 50% of total unsaturations at the lowest [M] values. An iPP sample prepared under starved catalyst conditions (2 mg of **2r**, **2r**/MAO = 2000, [M] → 0, toluene, 50 °C, 1 h) produced a powdery iPP with $M_n = 2000$ (from ^{13}C NMR) and the distribution of unsaturated end groups as vinylidene 39%, allyl 50%, *cis*-2-butenyl < 2%, the rest being composed of two different trisubstituted olefinic end groups at 4.9 ppm (ca. 2%, likely the isobutenyl end group originating from transfer/isomerization after a primary insertion) and at 5.2 ppm (7%). Clearly, for the more sterically demanding 4,7-dimethylindenyl ligand, methyl−methyl nonbonded interactions between the π-ligand and the growing chain end become relevant and force the methyl group of the last inserted unit toward the metal, in a conformation suitable for unimolecular β-methyl transfer. Our complete investigation on the kinetics of the different elementary steps in chain transfer reactions with both **1r** and **2r** will be reported in due time.

The decrease of *cis*-butenyl end groups with monomer concentration confirms that the mechanism of chain transfer is hydrogen transfer *to the monomer* after a secondary insertion ($R_{tMon} = k_{tMon}[C_s^*][M]$).

Inspection of molecular models accounts for this experimental evidence: nonbonded contacts are minimized for a *syn* placement of the CH_3 and polymer chain in the conformation leading to chain transfer to the

(35) Kashiwa, N.; Kioka, M. *Polym. Mater. Sci. Engin.* **1991**, *64*, 43. Kioka, M.; Mizuno, A.; Tsutsui, T.; Kashiwa, N. In *Catalysis in Polymer Synthesis*; Vandenberg, E. J., Salamone, J. C., Eds.; ACS Symposium Series 496; American Chemical Society: Washington, DC, 1992; p 72.
(36) Busico, V.; Cipullo, R.; Corradini, P. *Makromol. Chem.* **1993**, *194*, 1079.
(37) (a) Tsutsui, T.; Mizuno, A.; Kashiwa, N. *Polymer* **1989**, *30*, 428. (b) Kaminski, W.; Ahlers, A.; Möller-Lindenhof, N. *Angew. Chem., Int. Ed. Engl.* **1989**, *28*, 1216. (c) Resconi, L.; Piemontesi, F.; Franciscono, G.; Abis, L.; Fiorani, T. *J. Am. Chem. Soc.* **1992**, *114*, 1025.
(38) (a) Eshuis, J.; Tan, Y.; Teuben, J. H.; Renkema, J. *J. Mol. Catal.* **1990**, *62*, 277. (b) Eshuis, J.; Tan, Y.; Meetsma, A.; Teuben, J. H. *Organometallics* **1992**, *11*, 362. (c) Yang, X.; Stern, C. L.; Marks, T. J. *Angew. Chem., Int. Ed. Engl.* **1992**, *31*, 1375. (d) Mise, T.; Kageyama, A.; Miya, S.; Yamazaki, H. *Chem. Lett.* **1991**, 1525. (e) Kesti, M.; Waymouth, R. *J. Am. Chem. Soc.* **1992**, *114*, 3565. (f) Guo, Z.; Swenson, D.; Jordan, R. *Organometallics* **1994**, *13*, 1424. (g) Hajela, S.; Bercaw, J. E. *Organometallics* **1994**, *13*, 1147. (h) Yang, X.; Stern, C. L.; Marks, T. J. *J. Am. Chem. Soc.* **1994**, *116*, 10015. (i) Resconi, L.; Jones, R. L.; Albizzati, E.; Camurati, I.; Piemontesi, F.; Guglielmi, F.; Balbontin, G. *ACS Polym. Prepr.* **1994**, *35* (1), 663. (j) Resconi, L.; Jones, R. L.; Rheingold, A. L.; Yap, G. P. A. *Organometallics* **1996**, *15*, 998.
(39) Tsutsui, T.; Kashiwa, N.; Mizuno, A. *Makromol. Chem., Rapid Commun.* **1990**, *11*, 565.
(40) Shiono, T.; Soga, K. *Macromolecules* **1992**, *25*, 3356.

Scheme 4

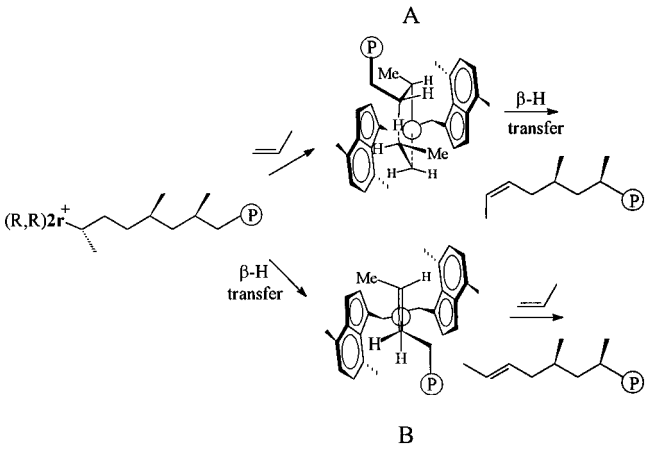

Scheme 5

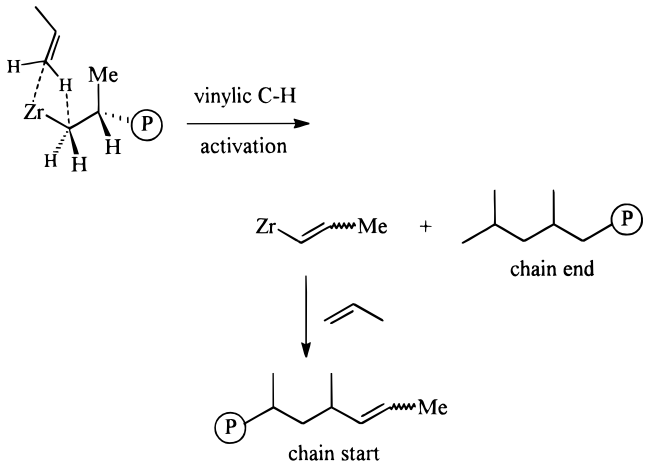

monomer after a secondary insertion with formation of a *cis*-2-butenyl end group (Scheme 4, path A).

The kinetic equivalent of such a mechanism, i.e., unimolecular methylene hydrogen transfer to the metal after a secondary insertion, with the olefin remaining coordinated to the zirconium cation and then released only upon associative exchange with a propene molecule, is less likely because in this instance a *trans*-2-butenyl end group would be expected (Scheme 4, path B).[41]

Another different chain transfer mechanism could be suggested, which would form an internal double bond: propene vinylic C−H activation with formation of a $ZrCH{=}CHCH_3$ initiating species (Scheme 5). Such a mechanism has been proposed in the case of ethylene polymerization with Cp_2ZrCl_2/MAO catalyst.[42,43]

However, propene vinylic C−H activation is ruled out by the absence of an equivalent amount of isobutyl groups and by comparison with the spectra of 4-methyl-*cis*-2-pentene and *cis*- and *trans*-2-octene (Table 9).

2m/MAO is only marginally active in the polymerization of propene, yielding low molecular weight aPP. ^{13}C NMR analysis reveals only isobutyl end groups,

Table 9. ^1H and ^{13}C NMR Chemical Shifts ($C_2D_2Cl_4$, 120 °C, Referenced to TMS) for *cis*-2-Butenyl Chain End and Model Molecules

	^{13}C NMR[a]			^1H NMR[b]
	CH_3—	—CH_2—	C=C	H H
trans-2-octene	17.65	32.62	124.62, 132.01	5.1−5.4
cis-2-octene	12.63	27.11	123.74, 131.24	5.1−5.4
cis-2-butenyl-PP	12.92	34.42	124.50, 129.67	5.18−5.38
cis-4-methyl-2-pentene	12.56		121.49, 138.89	5.0−5.2

[a] Middle peak of the $C_2D_2Cl_4$ triplet at 74.26 ppm. [b] $C_2D_2Cl_4$ at 5.75 ppm.

showing that the only mode of chain transfer is transfer to aluminum.[44]

2m is highly regiospecific, as no secondary insertions could be detected, either in the polymer chain or as end groups. As in the case of **2r**, **2m** seems to be able to reduce the extent of β-hydrogen transfer.

Experimental Section

General Procedures. All operations were performed under nitrogen by using conventional Schlenk-line techniques. Solvents were distilled from blue Na−benzophenone ketyl (THF), $LiAlH_4$ (Et_2O), CaH_2 (CH_2Cl_2), P_4O_{10} ($CHCl_3$), or $AliBu_3$ (hydrocarbons) and stored under nitrogen. Typical residual water content was 2 ppm. Indene (Aldrich) was distilled from CaH_2. 1,2-Dibromoethane (Aldrich) was stored over molecular sieves, Me_2SiCl_2 (Aldrich) was distilled prior to use, and Me_3SiCl (Aldrich) was used as received. MeLi (Aldrich), BuLi (Aldrich), and BOMAG (Schering) were used as received. KH (Aldrich, 35% w/w suspension in mineral oil) was diluted with hexane, stirred, transferred via Teflon cannula into a filter under nitrogen, washed with hexane, and dried in vacuo to a gray-white free-flowing powder (*caution: highly pyrophoric*!). All compounds were analyzed on an AC 200 Bruker spectrometer operating at 200.13 MHz for ^1H and 50.323 MHz for ^{13}C, by ^1H NMR ($CDCl_3$, referenced against the peak of residual $CHCl_3$ at 7.25 ppm) or ^{13}C NMR (broad band decoupling mode) ($CDCl_3$, referenced against the central line of $CDCl_3$ at 77.00 ppm). All NMR solvents were dried over $LiAlH_4$ and distilled before use. Preparation of the samples was carried out under nitrogen using standard inert-atmosphere techniques. Due to the low solubility of the zirconocenes, these samples were prepared as saturated solutions in 0.5 mL of solvent in a 5-mm NMR tube. Polymerization grade propene and hexane were received directly from the Montell Ferrara plant. MAO was a commercial product (Witco, 30% w/w in toluene) treated as previously recommended[44d] in order to remove most of the unreacted TMA. *rac*-Ethylenebis(1-indenyl)$ZrCl_2$ (**1r**) was prepared according to Collins[10d] and purified by CH_2Cl_2 extraction.[11] *rac*-Ethylenebis(1,2,3,4-tetrahydro-1-indenyl)-$ZrCl_2$ (*rac*-EBTHIZrCl_2)[45] and its *meso* isomer,[10c] *rac*-Me_2Si(1-indenyl)$_2ZrCl_2$,[46] and *rac*-Me_2Si(4,5,6,7-tetrahydro-1-indenyl)$_2ZrCl_2$[47] were prepared according to published procedures. The isomeric and chemical purities of all compounds were checked by ^1H NMR (Bruker 200 MHz, $CDCl_3$, signal-to-noise ratio 200, referenced against $CHCl_3$ at 7.25 ppm). All

(41) Grossman, R. B.; Davis, W. M.; Buchwald, S. L. *J. Am. Chem. Soc.* **1991**, *113*, 2321.
(42) Siedle, A. R.; Lamanna, W. M.; Olofson, J. M.; Nerad, B. A.; Newmark, R. A. In *Selectivity in Catalysis*; Davis, M. E., Suib, S. L., Eds.; ACS Symposium Series 517; American Chemical Society: Washington, DC, 1993; p 156.
(43) Woo, T. K.; Fan, L.; Ziegler, T. In *Ziegler Catalysts*; Fink, G., Mülhaupt, R., Brintzinger, H. H., Eds.; Springer-Verlag: Berlin, 1995; p 291.
(44) (a) Chien, J. C. W.; Wang, B. P. *J. Polym. Sci., A: Polym. Chem.* **1988**, *26*, 3089. (b) Chien, J. C. W.; Razavi, A. *J. Polym. Sci., A: Polym. Chem.* **1988**, *26*, 2369. (c) Chien, J. C. W.; Wang, B. P. *J. Polym. Sci., A: Polym. Chem.* **1990**, *28*, 15. (d) Resconi, L.; Bossi, S.; Abis, L. *Macromolecules* **1990**, *23*, 4489.
(45) Wild, F.; Wasiucionek, M.; Huttner, G.; Brintzinger, H.-H. *J. Organomet. Chem.* **1985**, *288*, 63.
(46) Herrmann, W.; Rohrmann, J.; Herdtweck, E.; Spaleck, W.; Winter, A. *Angew. Chem., Int. Ed. Engl.* **1989**, *28*, 1511.
(47) Welborn, H. U.S. Patent 5,314,973 to Exxon (1994).

compounds were also analyzed by ^{13}C NMR (50.3 MHz, $CDCl_3$, referenced against $CDCl_3$ at 77.00 ppm).

Polymerizations. Polymerization experiments were carried out in a 2-L stainless-steel autoclave (liquid monomer polymerizations) at constant pressure for 1 h and 50 (±1) °C. Stirring was kept at 800 rpm by means of a three-blade propeller.

Metallocene and MAO were precontacted for 10 min in toluene solution (10 mL) and then added to the monomer/solvent mixture at 48 °C. The polymerizations were quenched with CH_3OH; the polymers were isolated by distilling off the solvents under reduced pressure and dried at 50°C in vacuo overnight.

Polymer Analysis. Intrinsic viscosities were measured in tetrahydronaphthalene at 135 °C and converted into average viscosimetric molecular weights using the Mark−Houwink equation for iPP with $\alpha = 0.74$ and $K = 1.93 \times 10^{-4}$.[48]

Solution ^{13}C NMR spectra were run at 75.4 MHz on a Varian UNITY-300 NMR spectrometer. Samples were run as 15% solutions in $C_2D_2Cl_4$ at 130 °C. Chemical shifts are referenced to TMS using as a secondary reference the methyl peak of polypropene at 21.8 ppm. A total of 6000 transients were accumulated for each spectrum with a 12 s delay between pulses. Decoupling was always on during acquisition so the nuclear Overhauser enhancement was present. The carbon spectra were analyzed as previously described.[13] Solution ^1H NMR spectra were run at 130 °C in $C_2D_2Cl_4$ on a Bruker 500 spectrometer.

Synthesis of 1,2-Bis(4,7-dimethylindenyl)ethane. A 26.03 g amount (90% pure by ^1H-NMR, 163 mmol) of 4,7-dimethylindene and 500 mL of dried THF were placed in a 3-neck 1-L flask equipped with a 250-mL dropping funnel, under nitrogen atmosphere. After cooling of the solution to −70 °C, 143 mL of a 1.6 M hexane solution of butyllithium (229 mmol) was added, dropwise over 40 min. The so obtained suspension was allowed to warm to room temperature and stirred for 4 h (color changing from yellow to green and finally to brown-red, at which point a solution is obtained). After cooling of the solution to −70 °C, a solution containing 7.8 mL (17 g, 90.5 mmol) of 1,2-dibromoethane in 50 mL of THF was added dropwise with stirring. After the addition was complete, the reaction mixture was allowed to warm to room temperature and stirred overnight. A 0.5 mL volume of water was added, and the solvents were removed in vacuo, yielding a solid which was extracted with 500 mL of dichloromethane. After filtration the solvent was evaporated giving a sticky solid. To this solid was added 800 mL of ethyl alcohol, and the suspension was refluxed for 10 min. After 1 night at −20 °C a light brown solid separated and 10.1 g of this product was collected (fraction A). The mother liquor concentrated to 400 mL and kept at −20 °C overnight yielded 10.3 g of light brown solids (fraction B). GC−MS analysis of the two fractions A and B gave the following weight compositions.

A (10.1 g): 4,7-dimethylindene, 0.3%; spiro(cyclopropane-1,1′-4,7-dimethylindene), 0.6%; 1,2-bis(4,7-dimethylinden-1-yl)-ethane, 15.6%; 1-(4,7-dimethylinden-1-yl)-2-(4,7-dimethylinden-3-yl)ethane, 8.5%; 1,2-bis(4,7-dimethylinden-3-yl)ethane, 61.5%; 1,2-bis(4,7-dimethylindenyl)ethane, total isomers 85.6%.

B (10.3 g): 4,7-dimethylindene, 0.6%; spiro(cyclopropane-1,1′-4,7-dimethylindene), 2.0%; 1,2-bis(4,7-dimethylinden-1-yl)-ethane, 11.3%; 1-(4,7-dimethylinden-1-yl)-2-(4,7-dimethylinden-3-yl)ethane, 61.3%; 1,2-bis(4,7-dimethylinden-3-yl)ethane, 2.5%; 1,2-bis(4,7-dimethylindenyl)ethane, total isomers 75.1%.

Isolated yield: 64.5%. The mother liquor brought to dryness gave 21.6 g of a yellow-orange paste which contained (by GC) 13.5% of spiro(cyclopropane-1,1′-4,7-dimethylindene) and 32.8% of 1,2-bis(4,7-dimethylindenyl)ethane isomers.

Synthesis of 1,2-Bis(1-(trimethylsilyl)-4,7-dimethyl-3-indenyl)ethane (EBDMI(TMS)$_2$). A 103.8 g amount of 1,2-bis(4,7-dimethylindenyl)ethane (MW 314.108 g/mol, 331 mmol) was slurried in 680 mL of THF in a 1 L flask equipped with a stirring bar. This suspension was added in small aliquots over 30 min at room temperature in a 2 L flask equipped with reflux condenser, thermometer, and mechanical stirrer, containing 29.48 g of KH (MW 40.11, 735 mmol) and 205 mL of THF. The reaction was slightly exothermic (T_{max} = 43 °C) with evolution of hydrogen. At the end of the addition the so obtained suspension was stirred for 2 h, yielding a dark green solution. In a second 2 L flask equipped with thermometer, mechanical stirrer, and dropping funnel was placed 93.2 mL of Me_3SiCl (MW 108.64, d = 0.856, 734 mmol) and 210 mL of THF. The dark green solution of the potassium salt was added dropwise (2 h, slightly exothermic reaction, T_{max} = 30 °C), and at the end of the addition the mixture was stirred for 44 h, yielding a brown-orange milk. The reaction was monitored by GC: after 16 h the reaction was complete. The mixture was then treated with water (200 mL) while stirring and then NaCl to induce phase separation. The organic layer was dried over Na_2SO_4, filtered, and brought to dryness: a light brown solid was obtained (142.8 g; theoretical 151.5 g), yield 94.3%.

The reverse addition (TMSCl on the dipotassium salt of 1,2-bis(4,7-dimethylindenyl)ethane) gave the same results: 10 g of 1,2-bis(4,7-dimethylindenyl)ethane (32 mmol) was slurried in 65 mL of THF in a 250 mL flask with a stirring bar. This suspension was slowly siphoned at room temperature into a 250 mL flask containing 2.84 g of KH (71 mmol) and 20 mL of THF and equipped with reflux condenser, thermometer, and mechanical stirrer. The reaction is slightly exothermic (T_{max} = 35 °C) with evolution of hydrogen. At the end of the addition the suspension was stirred for 2 h, at the end of which time a dark green solution was obtained. To this solution were slowly added (30 min) 9 mL of Me_3SiCl (71 mmol) in 20 mL of THF (slightly exothermic reaction, T_{max} = 38 °C). At the end of the addition the suspension was stirred for 7 h, yielding a yellow-orange milk. The reaction was monitored by NMR (40 mg in $CDCl_3$). After 1 h the reaction was complete. After 7 h the mixture was treated with 50 mL of brine while stirring. Phase separation was observed. The organic layer was dried over Na_2SO_4, filtered, and then brought to dryness: a light brown solid was obtained (11.87 g, theoretical 14.6 g), yield 94.2%.

1,2-Bis(1-(trimethylsilyl)-4,7-dimethyl-3-indenyl)ethane Isomer Separation by Pentane Extraction. A 105.3 g amount of 1,2-bis(1-(trimethylsilyl)-4,7-dimethyl-3-indenyl)-ethane was extracted with 0.5 L of pentane on a γ frit with side arm for continuous extraction, until all the reddish material was removed. The filtrate (dark red) brought to dryness yields 60.3 g of dark red product. ^1H NMR ($C_2D_2Cl_4$ 120 °C): *rac*/*meso* ca. 9/1. The ochre residue was continuously extracted with refluxing hexane. (A dark brown residue (solubile in acetone) together with some white material (insoluble in acetone) is left on the frit.) The product crystallizes in the receiving flask. After cooling to room temperature and resting overnight, the mother liquor was eliminated and the crystalline product (37.4 g) was brought to dryness in vacuo. ^1H NMR ($C_2D_2Cl_4$ 120 °C): pure *meso*.

The spectra of EBDMI(TMS)$_2$ in $CDCl_3$ at room temperature do not show splitting of peaks due to the different diastereoisomers. To allow for peak separation, the product is dissolved in $C_2D_2Cl_4$ and the spectrum acquired at 120 °C.

^{13}C NMR (ppm, $C_2D_2Cl_4$, 50.3 MHz, 120 °C): 146.83 (C), 143.24 (C), 142.27 (C), 131.69 (CH), 129.44 (C), 128.44 (C), 128.23 (CH), 125.74 (CH), 44.06 (CH), 31.71 (CH_2-*rac*), 31.54 (CH_2-*meso*), 20.22 (CH_3), 20.01 (CH_3), −0.41 ($SiCH_3$)$_3$).

***meso*-EBDMI(TMS)$_2$.** ^1H NMR (ppm, $C_2D_2Cl_4$, 200 MHz, 120 °C): 6.8−6.6 (m, 4H), 6.23 (bs, 2H), 3.31 (bs, 2H), 2.99 (s, 4H), 2.42 (s, 6H), 2.18 (s, 6H), −0.22 (s, 18H).

***rac*-EBDMI(TMS)$_2$.** ^1H NMR (ppm, $C_2D_2Cl_4$, 200 MHz, 120 °C): 6.8−6.6 (m, 4H), 6.25 (bs, 2H), 3.32 (bs, 2H), 2.99 (s, 4H), 2.40 (s, 6H), 2.18 (s, 6H), −0.20 (s, 18H).

Synthesis of 2m via *meso*-1,2-Bis(1-(trimethylsilyl)-4,7-dimethyl-3-indenyl)ethane. A 37.4 g amount of *meso*-

(48) Moraglio, G.; Gianotti, G.; Bonicelli, U. *Eur. Polym. J.* **1973**, *9*, 693.

$EBDMI(TMS)_2$ (81 mmol), 200 mL of CH_2Cl_2, and 19.0 of $ZrCl_4$ (81 mmol) were placed under nitrogen in a 500 mL flask equipped with a stirring bar. The mixture was stirred for 4 h at room temperature, and a dark green suspension was obtained. The reaction was stopped by removing the solvent in vacuo: a dark green free-flowing powder was obtained. (The NMR analysis shows the presence of **2m** and unidentified impurities.) The powder was placed on a frit and washed with THF until the washing was bright yellow (75 × 4 mL). After drying in vacuo, 31.3 g (80%) of light yellow powder was obtained. The ^1H NMR analysis shows the presence of pure **2m**.

Synthesis of 2r via *rac*-1,2-Bis(1-(trimethylsilyl)-4,7-dimethyl-3-indenyl)ethane. A 1.16 g amount of $ZrCl_4$ (5.0 mmol), 21 mL of CH_2Cl_2, and 2.28 g of $EBDMI(TMS)_2$ (5.0 mmol, *rac*:*meso* = 90:10) were placed in a 100 mL Schlenk tube with a stirring bar and stirred at room temperature for 3 h. A brown-yellow suspension was obtained. The reaction was stopped by removing the solvent in vacuo: a brown-yellow free-flowing powder was obtained (the NMR analysis shows the presence of **2r** + ca. 10% **2m** and unidentified impurities). The powder was rapidly washed with EtOH (5 mL) and Et_2O (5 × 2 mL). The residue was dried in vacuo yielding 1.23 g (52%) of product which was completely soluble in toluene. ^1H NMR shows the presence of **2r** (92%) + **2m** (8%).

***rac*- and *meso*-Ethylenebis(4,7-dimethyl-1-indenyl)-$ZrCl_2$ (Comparison).** The Zr complexes were also prepared by applying the procedure used by Buchwald for the preparation of $EBIZrCl_2$.[10c] A suspension of 1,2-bis(4,7-dimethylindenyl)ethane (10 g, 31.8 mmol) in THF (80 mL) was added via cannula to a stirred suspension of KH (2.82 g, 70.3 mmol) in THF (160 mL). After hydrogen evolution had subsided the resulting brownish solution was separated from excess KH. This solution and a solution of $ZrCl_4(THF)_2$ (12 g, 31.8 mmmol) in THF (250 mL) were both added dropwise via cannula to a flask containing rapidly stirring THF (50 mL) over 3 h. A yellow solution and a precipitate formed. After removal of the solvent in vacuo, the orange-yellow residue (mixture of *rac* and *meso* isomers, 2.33:1 by ^1H NMR) was extracted with CH_2Cl_2, until all orange product had dissolved. The yellow solid resulted to be a single stereoisomer (*meso*, 1.7 g 11.3% yield); evaporation of CH_2Cl_2 from the orange solution gave 4.9 g (32.5% yield) of an orange solid corresponding to a mixture of 93.7% *rac* and 6.3% *meso* isomers. Crystals suitable for X-ray diffraction studies were obtained by cooling concentrated solutions enriched in either isomer (*rac* isomer, toluene, −20 °C, orange crystals; *meso* isomer, chloroform, −20 °C, yellow crystals).

***rac*- and *meso*-(Dimethylsilyl)bis(4,7-dimethyl-1-indenyl)$ZrCl_2$ ($Me_2Si(4,7\text{-}Me_2Ind)_2ZrCl_2$).** Dimethylbis(4,7-dimethyl-3-indenyl)silane was prepared by the following procedure: 4,7-dimethylindene (40.2 g, 281 mmol) was dissolved in ether and the solution cooled to 0 °C. *n*-Butyllithium (1.6 M in hexane, 176 mL, 281 mmol) was added dropwise over 1 h. After being warmed to room temperature and stirred for 2 h, the obtained slurry was added dropwise to dichlorodimethylsilane (18 g, 140 mmol) in ether (60 mL). The mixture was stirred for 13 days, and then water (120 mL) was added maintaining the internal temperature at 25 °C. The organic phase was collected, washed with water (2 × 120 mL), and dried on Na_2SO_4. The solvent was removed by vacuum evaporation to provide 38 g of orange oil which contained 86.5 mol % of the target product and 13.5 mol % of unreacted 4,7-dimethylindene.

A 32.33 g amount of this oil was dissolved in THF (100 mL), and *n*-butyllithium (2 M in pentane, 100 mL, 200 mmol) was added dropwise at room temperature over 45 min. After being stirred for 3 h the solvent was removed in vacuo and the solid was filtered and washed copiously with Et_2O. A 16.57 g amount of the dilithium salt of dimethylbis(4,7-dimethyl-3-indenyl)silane, free of 4,7-dimethylindene, was obtained. The dilithium salt was dissolved in THF (200 mL). This solution and a solution of $ZrCl_4(THF)_2$ (17.5 g, 46.39 mmol) in THF (200 mL) were both added dropwise at room temperature to a flask containing rapidly stirring THF (50 mL) over 4 h. A dark brown solution was formed, and after 18 h at room temperature the solvent was removed in vacuo and the orange-brown residue treated with Et_2O: an orange solid was formed and collected by filtration yielding 3 g (15% yield) containing 83% of *rac* isomer and 17% of *meso* isomer.

***rac*-$Me_2Si(4,7\text{-}Me_2Ind)_2ZrCl_2$.** ^1H NMR (200 MHz, $CDCl_3$): δ 7.06 (d, J = 3.5 Hz, 2 H, C_5 ring), 7.00 (d, J = 6.2 Hz, 2 H, C_6 ring), 6.84 (d, J = 6.2 Hz, 2 H, C_6 ring), 6.19 (d, J = 3.5 Hz, 2 H, C_5 ring), 2.51 (s, 6 H, Ar methyl) 2.38 (s, 6 H, Ar methyl) 1.14 (s, 6 H, Si methyl).

***meso*-$Me_2Si(4,7\text{-}Me_2Ind)_2ZrCl_2$.** ^1H NMR (200 MHz, $CDCl_3$): δ 7.07 (d, J = 3.6 Hz, 2 H, C_5 ring), 6.85 (br s, 4 H, C_6 ring), 6.73 (d, J = 3.6 Hz, 2 H, C_5 ring), 2.48 (s, 6 H, Ar methyl), 2.35 (s, 6 H, Ar methyl), 1.25 (s, 6 H, Si methyl), 1.11 (s, 6 H, Si methyl).

***rac*-(Dimethylsilyl)bis(1-indenyl)$ZrCl_2$ (*rac*-$Me_2Si(Ind)_2ZrCl_2$).** Dimethylbis(indenyl)silane was prepared with the following procedure: Indene (29.9 g, 257 mmol) was dissolved in THF (300 mL) and the solution cooled to −80 °C. *n*-Butyllithium (1.6 M in hexane, 170 mL, 272 mmol) was added dropwise over 30 min. After being warmed to room temperature and stirred for 3 h, a dark red solution was obtained. This solution was added dropwise to dichlorodimethylsilane (16.6 g, 129 mmol) in THF (200 mL) at 0 °C. The mixture was warmed to room temperature, stirred for 16 h, and then quenched with water (50 mL). The organic phase was collected and dried over Na_2SO_4, and the solvent was removed in vacuo giving a red oil. Volatiles were eliminated by warming the oily residue to 50 °C in vacuo. An 18.8 g (50.6% yield) amount of product was obtained as a mixture of three double-bond isomers. ^1H NMR (200 MHz, $CDCl_3$): δ 7.65−7.40 (m), 7.36−7.05 (m), 7.02−6.85 (m), 6.65 (m), 6.46 (m), 3.65 (br s), 3.50 (br s), −0.04 (s), −0.27 (s), −0.45 (s).

The synthesis of the complex is a slightly modified literature procedure.[47] Dimethylbis(indenyl)silane (9.4 g, 32.59 mmol) was dissolved in THF (70 mL) and the solution cooled at −78 °C. *n*-Butyllithium (1.6 M in hexane, 40.7 mL, 65.2 mmol) was added dropwise. The dark green solution was warmed to room temperature and stirred for 1 h (turned red). This solution was added dropwise (room temperature, 1 h) to a suspension of $ZrCl_4$ $(THF)_2$ (12.4 g, 32.87 mmol), and the mixture was allowed to stir overnight. A yellow-orange precipitate formed; the solution was concetrated to half-volume, and the solid was filtered off, washed with 10 mL of cold (−20 °C) THF and 20 mL of Et_2O, and finally dried in vacuo. A 4.97 g amount of orange microcrystalline solid (34% yield) was obtained. ^1H NMR (200 MHz, $CDCl_3$): δ 7.60 (d, 2 H), 7.50 (d, 2H), 7.37 (t, 2 H), 7.09 (t, 2 H), 6.92 (d, 2 H), 6.10 (d, 2 H), 1.13 (s, 6 H).

X-ray Structure Determination and Refinements. Crystal data and experimental conditions for compounds *meso*-1,2-bis(1-(trimethylsilyl)-4,7-dimethyl-3-indenyl)ethane and **2r**,**m** are reported in Table 10. Unit cell parameters were determined by least-squares fit of the setting angles of 25 intense reflections having a θ value in the range 10.0−14.0°. The intensity data were recorded on an Enraf-Nonius CAD-4 automated diffractometer at room temperature using the scan conditions and sampling the reciprocal lattice as reported in Table 10.

The crystal stability was checked by monitoring three standard reflections every 60 min. The diffracted intensities were corrected for Lorentz, polarization, and background effects. An empirical absorption correction was applied according to the method developed by North *et al.* based on ψ scans (ψ 0−360°, every 10°) of three reflections having χ values near 90°.[49] Scattering factors for neutral atoms and anoma-

(49) North, A. C. T.; Phillips, D. C.; Scott Mathews, F. *Acta Crystallogr.* **1968**, *A24*, 351.

Table 10. Summary of Crystal Data and Data-Collection/Analysis Parameters

	meso-EBDMI(TMS)$_2$	**2r**	**2m**
formula	$C_{30}H_{42}Si_2$	$C_{24}H_{24}Cl_2Zr$	$C_{24}H_{24}Cl_2Zr$
M_n	458.8	474.6	474.6
cryst system	monoclinic	monoclinic	monoclinic
space group	$P2_1/c$ (No. 14)	$I2/c$ (No. 15)	$P2_1/c$ (No. 14)
a/Å	6.427(1)	11.685(2)	11.616(1)
b/Å	17.439(8)	12.878(3)	11.615(1)
c/Å	12.541(2)	14.143(2)	15.289(1)
β/deg	96.21(1)	102.37(1)	102.98(1)
V/Å^3	1397(1)	2079(1)	2010(1)
Z	2	4	4
D_c/g cm^{-3}	1.090	1.516	1.568
F(000)	500	968	968
cryst dimens/mm	0.30 × 0.20 × 0.20	0.20 × 0.15 × 0.07	0.25 × 0.15 × 0.15
μ(Mo Kα)/cm^{-1}	1.4	7.8	8.1
min rel transm factor	0.96	0.96	0.92
no. of reflcns for ψ-scan	3	3	3
θ range/deg	3−25	3−27	3−27
scan mode	ω	ω	ω
scan range/deg	0.8 + 0.35 tan θ	0.8 + 0.35 tan θ	0.8 + 0.35 tan θ
required $\sigma(I)/I$	0.01	0.01	0.01
max scan time/s	70	70	70
octants of recipr space collcd	$\pm h,k,l$	$\pm h,k,l$	$\pm h,k,l$
cryst decay	2%	No	No
no. of collcd reflcns (at RT)	2527	2365	4579
no. of unique obsd reflns [$I > 3\sigma(I)$]	1676	1947	3579
no. of refined params	191	126	340
weights (a, b)	0.0783, 0.2837[a]	1.512, 0.003259[b]	1.0871, 0.000617[b]
max shift/error	<0.01	<0.01	<0.01
R[c]	0.041	0.032	0.019
R'	0.115[d]	0.037[e]	0.022[e]
max peak diff Fourier map/e Å^{-3}	0.20	0.45	0.24

[a] $w = 1/[\sigma^2(F_o^2) + (aP)^2 + bP]$, where $P = (F_o^2 + 2F_c^2)/3$. [b] $w = a/(\sigma^2(F_o) + bF_o^2)$. [c] $R = \sum(|F_o - k|F_c||)/\sum F_o$. [d] $R' = [\sum w(F_o^2 - F_c^2)^2/\sum wF_o^4]^{1/2}$. [e] $R' = [\sum w(F_o - k|F_c|)^2/\sum wF_o^2]^{1/2}$.

lous dispersion corrections for scattering factors were taken from refs 50 and 51, respectively.

The structures were solved by standard Patterson and Fourier methods and refined by full-matrix least squares against F_o^2 (*meso*-1,2-bis(1-(trimethylsilyl)-4,7-dimethyl-3-indenyl)ethane) or F_o (**2r**,**m**). Weights were assigned to individual observations according to the formulas reported on Table 10. Anisotropic thermal parameters were assigned to all non-hydrogen atoms. Hydrogen atom parameters were refined for the **2m** derivative while for *meso*-1,2-bis(1-(trimethylsilyl)-4,7-dimethyl-3-indenyl)ethane and **2r** the hydrogen atoms were placed in idealized positions (C−H 0.95 Å) and refined riding on their parent atom with a common (refined) isotropic thermal parameters.

The structure of **2r** was affected by a slight disorder of the ethylenebis(4,7-dimethyl-1-indenyl) ligand, which seems to be due to some conformational freedom around the ethylene hinge. We were not able to refine a consistent disordered model (in a noncentrosymmetric subgroup of $I2/c$), possibly because of the closeness of the separated individuals. Hence, in order to favor the convergence toward a stereochemical significant result, the chemically equivalent C−C interactions within the indenyl ligands were restrained (with σ of 0.005 Å) to have similar bond distances. The disorder is nevertheless still manifested by the moderately large thermal ellipsoids of the carbon atoms and by the unreasonably short C(8)−C(8′) bond distances. In keeping with the observed disorder, even if it does not explain it, the "ordered" stereoisomer is packed more efficiently than the "disordered" ones (*i.e.* **2m** has a smaller U/Z values than **2r**).

The final values of the agreement indices, R and R', and of maximum residuals in the final difference Fourier synthesis are reported in Table 10. The final positional parameters are reported in the Supporting Information for *meso*-1,2-bis(1-(trimethylsilyl)-4,7-dimethyl-3-indenyl)ethane and **2r**,**m**, respectively. All the calculations were performed on a Personal IRIS 35 using SHELXL93 (*meso*-1,2-bis(1-(trimethylsilyl)-4,7-dimethyl-3-indenyl)ethane) or SHELX76 (**2r**,**m**).[52]

Conclusions

We have presented here a new, high-yield and diastereoselective synthesis of the known [ethylenebis(4,7-dimethyl-1-indenyl)]zirconium dichloride, which is independent from the relative stability of the two isomers. In particular, this method is quite useful for the synthesis of the *meso* isomer, which has been previously found by some of us to be a quite useful precatalyst in the synthesis of high molecular weight ethylene-based polyolefins. Although the use of TMS-derivatized, bridged bis(cyclopentadienyl) ligands in the synthesis of *ansa*-zirconocenes is less general than we had hoped, we are currently working on its application to other, more demanding complexes.

In the racemic isomer **2r**, substituting H for methyl on the 4,7 positions of the indenyl moiety causes a higher rigidity of the complex in solution in comparison to the unsubstituted parent complex **1r**: at 52 °C, almost 90% of the molecules are in the Π conformation. The ethylenebis(4,7-dimethylindenyl) ligand in the *meso* isomer **2m** is noticeably distorted toward the axis

(50) Cromer, D. T.; Waber, J. T. *International Tables for X-Ray Crystallography*; The Kynoch Press: Birmingham, U.K., 1974; Vol. 4, Table 2.2.b (present distributor: Kluwer Academic Publishers, Dordrecht, The Netherlands).

(51) Cromer, D. T. *International Tables for X-Ray Crystallography*; The Kynoch Press: Birmingham, U.K., 1974; Vol. 4, Table 2.3.1 (present distributor: Kluwer Academic Publishers, Dordrecht, The Netherlands).

(52) Sheldrick, G. M. SHELXL93, Program for crystal structure determination. Univ. of Goettingen, Germany, 1994. Sheldrick, G. M. SHELX76, Program for crystal structure determination. Univ. of Cambridge, England, 1976.

bisecting the Cl−Zr−Cl angle, while the unsubstituted parent complex **1m** showed no such distortion.

We have also provided a further example of the close correlation between ligand structure and performance of the zirconocene catalyst in olefin polymerization. Especially, we have shown that the end group structure, hence the mechanism of chain transfer reactions, can be modified to a large extent by varying the substitution on the π-ligands. We have elucidated the mechanism of the chain transfer to the monomer after a secondary propene unit: this transfer produces only *cis*-2-butenyl-terminated iPP with both [ethylenebis(1-indenyl)]$ZrCl_2$/MAO and [ethylenebis(4,7-dimethyl-1-indenyl)]$ZrCl_2$/MAO. The selectivity toward this transfer reaction is well above 90% with the latter catalyst when liquid propene is polymerized at 50 °C.

Acknowledgment. The first synthesis of bis(4,7-dimethylindenyl)ethane was carried out by A. Coassolo at the Istituto G. Donegani in 1991. Prof. I. E. Nifant'ev, with his work on the related bis(trialkylstannyl) derivatives and helpful discussions, has been instrumental in the development of the bis(trimethylsilyl) route to the synthesis of *rac*- and *meso*-EBDMI$ZrCl_2$. We are indebted to Prof. G. Guerra and Prof. R. Grubbs for helpful discussions on the chain transfer mechanisms. We thank M. Colonnesi for the polymerization experiments, Dr. F. Testoni for the GC−MS analysis of the organic intermediates and ligands, A. Marzo for the viscosity measurements, O. Sudmeijer for the ^1H NMR polymer spectra, and G. McClelland for the ^{13}C NMR polymer spectra.

Supporting Information Available: Full listings of bond distances and bond angles, anisotropic thermal parameters, and atom coordinates and *U* values and COSY and NOESY spectra of **2r**,**m** and experimental and calculated spectra of the ethylene bridge region of **2r** in $C_2D_2Cl_4$ at different temperatures (20 pages). Ordering information is given on any current masthead page.

OM9604233